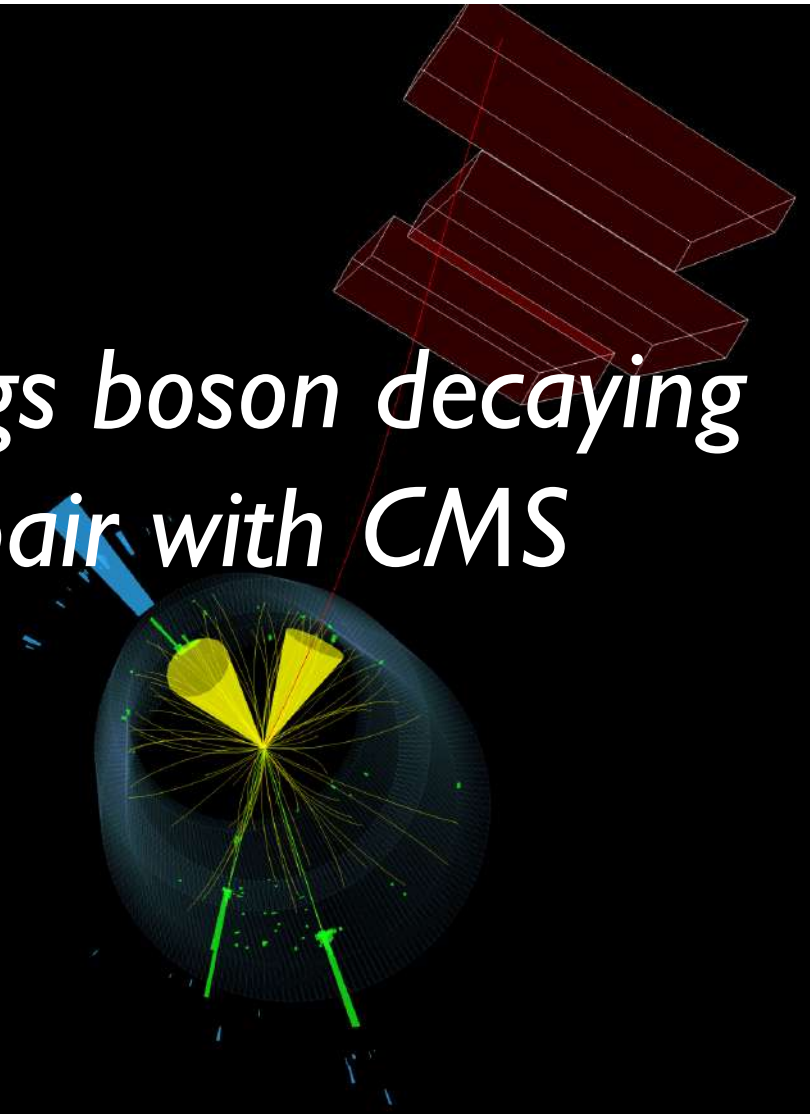


RWTHAACHEN
UNIVERSITY

Direct search for the SM Higgs boson decaying to a charm quark-antiquark pair with CMS

Luca Mastrolorenzo¹
on behalf of the CMS Collaboration

IRN Terascale 2022 Bohn
28th March 2022

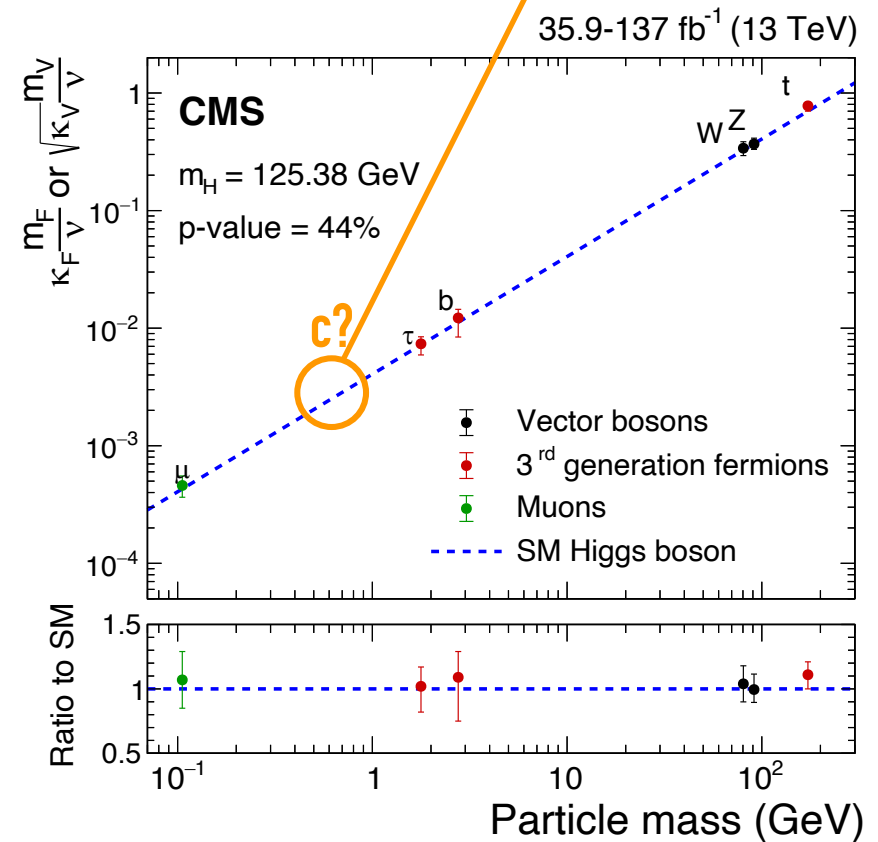
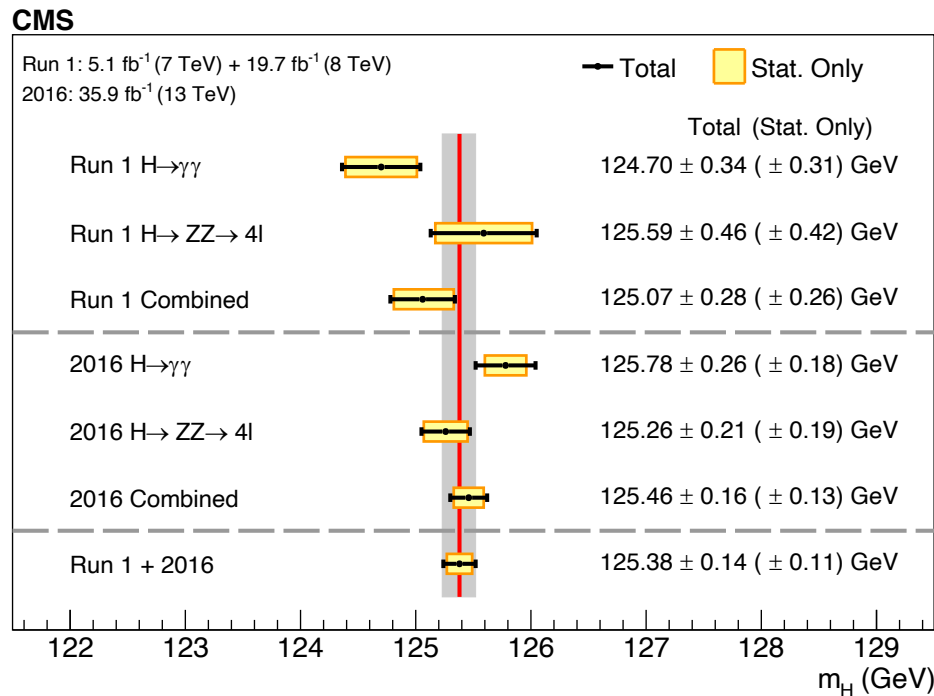


¹ Rheinisch-Westfälische Technische Hochschule (RWTH) Aachen

Understanding the Higgs boson

- Discovery of the Higgs boson in 2012: A new chapter of particle physics
- Tremendous progress in our understanding of the Higgs boson in the past ten years

- Probing Higgs coupling to 2nd generation quarks
- BSM effects enhanced given small value of SM κ_c

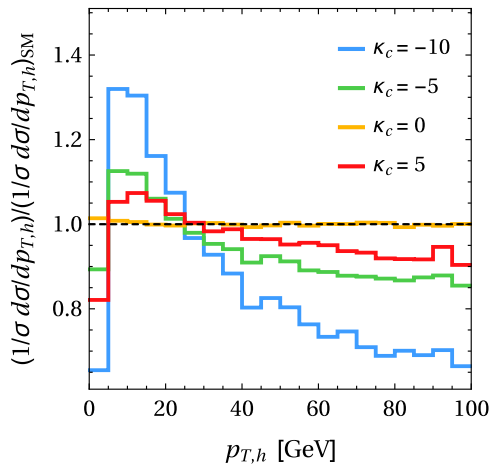


Probing the Higgs-charm coupling

Several methods explored by CMS to probe the Higgs-charm Yukawa coupling (y_c)

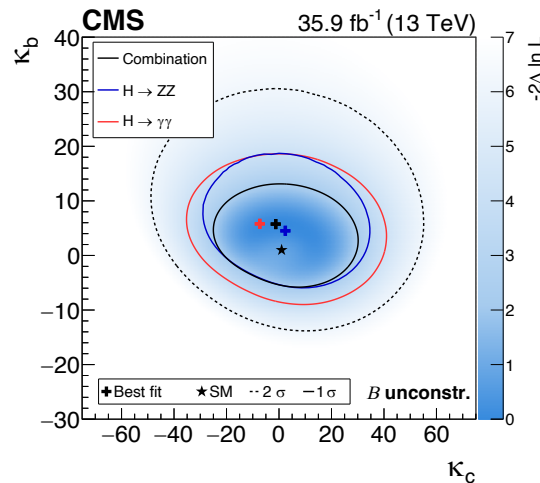
Indirect constraint from Higgs kinematics

Phys. Rev. Lett. 118, 121801



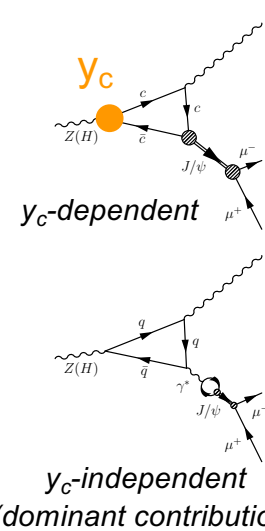
Variation of $p_T(H)$ shape as a function $\kappa_c = y_c/y_c^{SM}$

Phys. Lett. B 792 (2019) 369

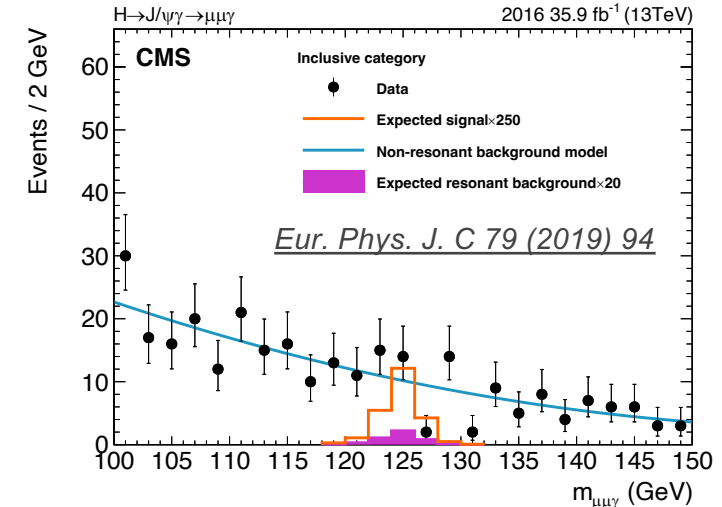


$-33 < \kappa_c < 38$ (obs.)
 $-31 < \kappa_c < 36$ (exp.)

Search for exclusive $H \rightarrow J/\Psi \gamma$ decays



Phys.Rev.D 90 (2014) 11, 113010
JHEP 08 (2015) 012
Phys.Rev.D 95 (2017) 5, 054018
Phys.Rev.D 100 (2019) 5, 054038



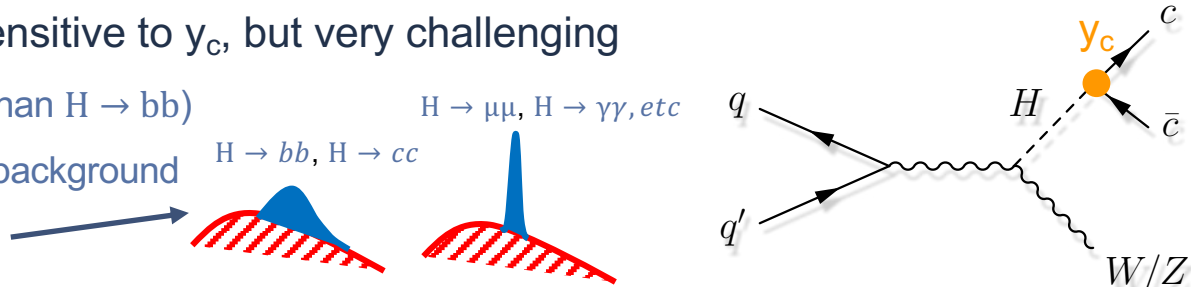
$\mathcal{B}(H \rightarrow J/\Psi \gamma) < 220x \text{ SM(obs.)}$
 $\mathcal{B}(H \rightarrow J/\Psi \gamma) < 170x \text{ SM(exp.)}$
 Roughly translates to $\kappa_c < O(100)$

Corresponding ATLAS analyses: [ATLAS-CONF-2022-002](#); *Phys. Lett. B* 786 (2018) 134. 3

Direct search for $H \rightarrow cc$

Search for $H \rightarrow cc$ decays: directly sensitive to y_c , but very challenging

- Quite small branching ratio (x20 smaller than $H \rightarrow bb$)
- QCD (reducible) and V+jets (irreducible) background
- Relatively poor invariant mass resolution
- charm quark identification + improvement of mass resolution play key roles



Main backgrounds

- V + jets, single and pair production of top quarks, dibosons, $VH(H \rightarrow bb)$

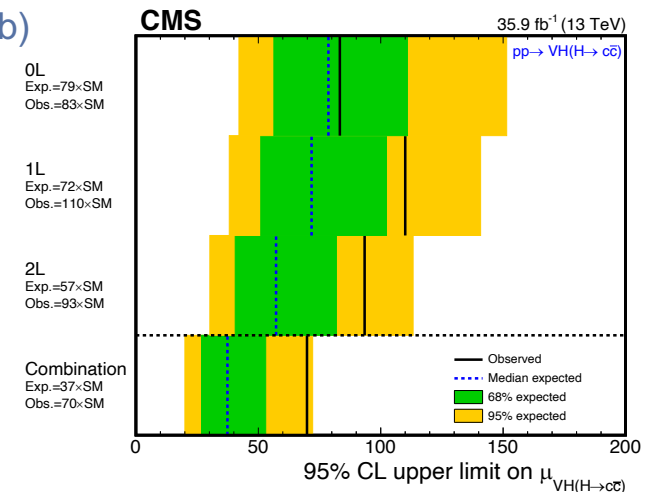
Exploit associated VH production (V = W, Z)

- Leptonic decays of V → handle to trigger events
- Boost of V → Reduce backgrounds
- Three channels: $Z \rightarrow \nu\nu$ (0L), $W \rightarrow \ell\nu$ (1L), $Z \rightarrow \ell\ell$ (2L) [$\ell = e, \mu$]

Previous result (36 fb^{-1}): [JHEP 03 (2020) 131]

Today: result with the full Run 2 data set (138 fb^{-1})

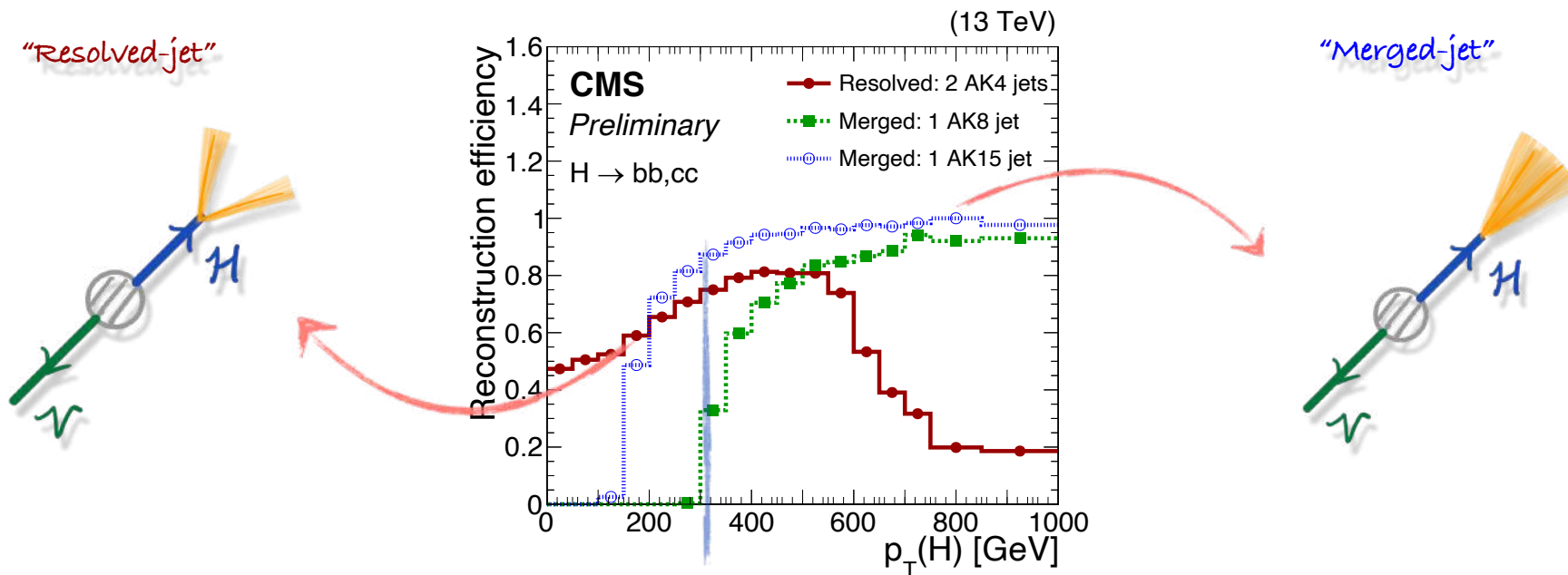
JHEP 03 (2020) 131



Corresponding ATLAS analysis: [arXiv:2201.11428](https://arxiv.org/abs/2201.11428). See also recent [LHC seminar](#) by A. Chisholm.

Analysis overview

□ $\Delta R(c, \bar{c}) \sim 2m(H)/p_T(H) \rightarrow$ Two complementary approaches for Higgs boson candidate reconstruction



Resolved-jet topology

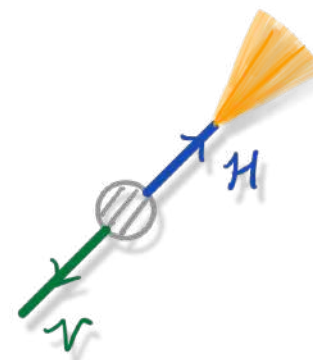
- reconstructs $H \rightarrow cc$ decay with two small-R jets ($R=0.4$, “AK4”)
- probes the bulk (>95%) of the signal phase space

Merged-jet topology

- reconstructs $H \rightarrow cc$ decay with one large-R jets ($R=1.5$, “AK15”)
- small signal acceptance (<5%) but higher purity
- better exploits the correlation between the two charm quarks

\rightarrow The two topologies are made orthogonal via presence of AK15 jet with $p_T > 300$ GeV

Merged-jet topology



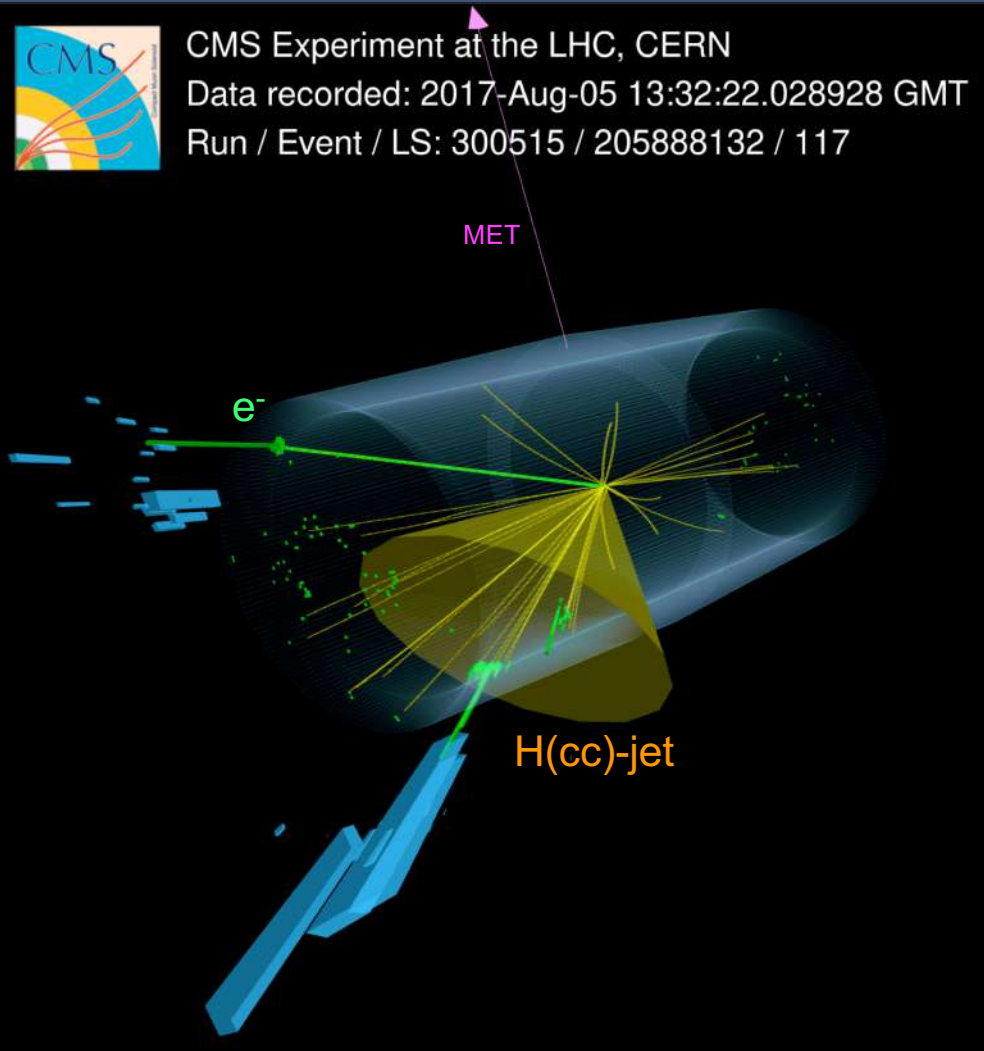
Overview of the merged-jet topology



CMS Experiment at the LHC, CERN

Data recorded: 2017-Aug-05 13:32:22.028928 GMT

Run / Event / LS: 300515 / 205888132 / 117



□ Higgs candidate reconstruction

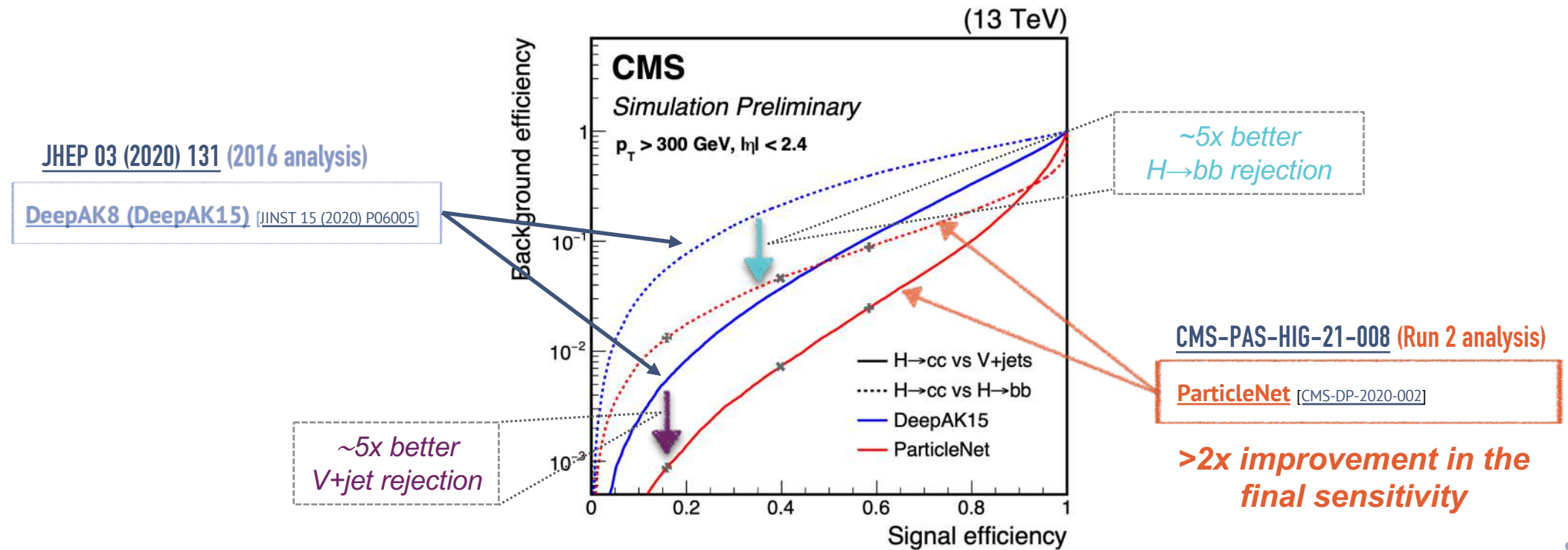
- Select one AK15-jets with the highest p_T as $H \rightarrow cc$ jet
- Identification of $H \rightarrow cc$ using ParticleNet tagger (dedicated calibration+mass sculpting mitigation)
- Dedicated cc-jet mass regression for improved cc-jet mass scale and resolution

□ Analysis strategy (three channels: 0L, 1L, 2L)

- Control regions for background normalizations
- Kinematic-BDT + cc-tagger score used for categorization
- Fit to soft-drop mass

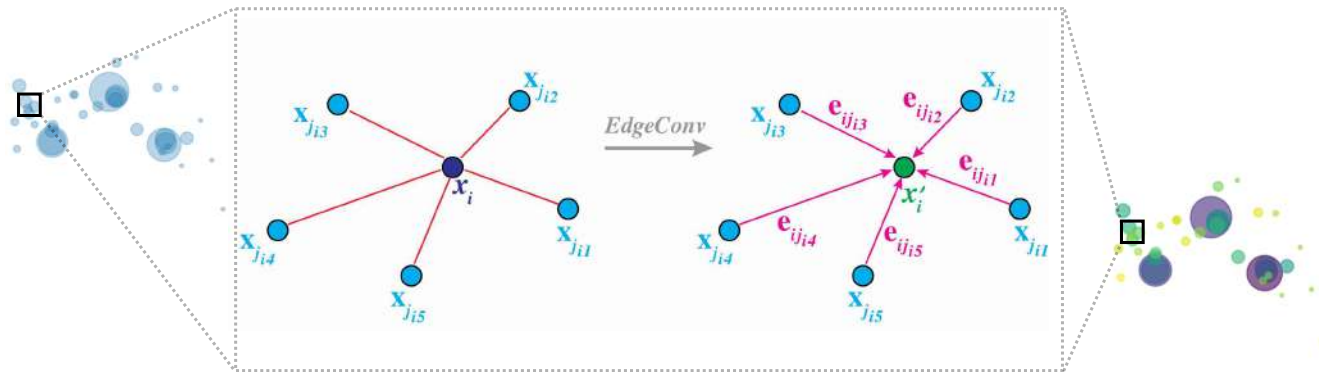
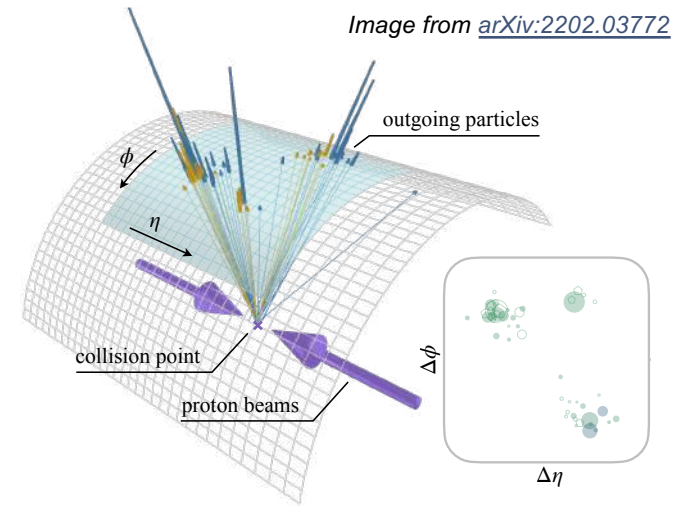
H → cc identification

- ❑ Merged-jet topology: Higgs boson candidate reconstructed via a single large-R jet ($p_T > 300$ GeV)
- ❑ **ParticleNet** tagger used to identify H → cc decay → Large improvement vs previous techniques
- ❑ Multi-class DNN boosted jet classifier → Trained targeting hadronic decays of a spin-0 particle X ($X \rightarrow bb, cc$)



ParticleNet architecture

- New jet representation: “particle cloud”
 - treating a jet as an unordered set of particles, distributed in the $\eta - \phi$ space
- ParticleNet [[Phys.Rev.D 101 \(2020\) 5, 056019](#)]
 - graph neural network architecture adapted from DGCNN [[arXiv:1801.07829](#)]
 - permutation-invariant architecture leads to significant performance improvement

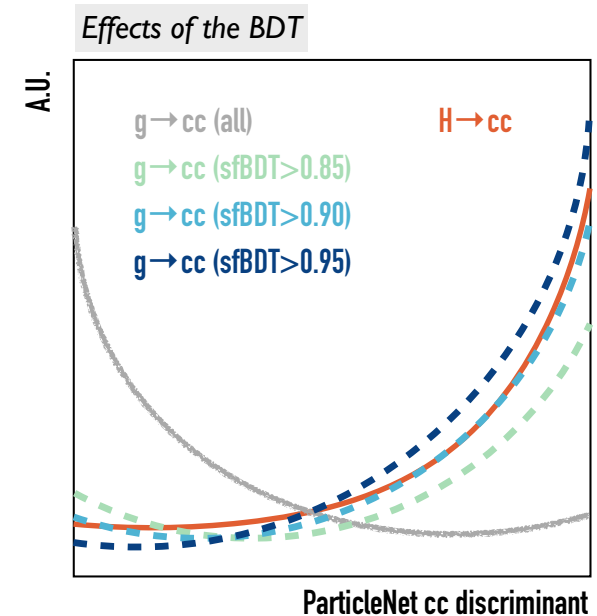
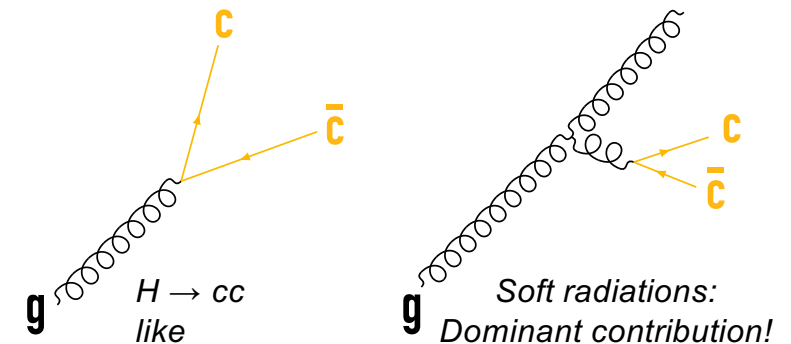


Performance on top quark tagging benchmark
[[SciPost Phys. 7, 014 \(2019\)](#)]

	$1/\epsilon_b$ at $\epsilon_s = 30\%$
ResNeXt-50	1147 ± 58
P-CNN	759 ± 24
PFN	888 ± 17
ParticleNet-Lite	1262 ± 49
ParticleNet	1615 ± 93

Calibration of the cc-tagger

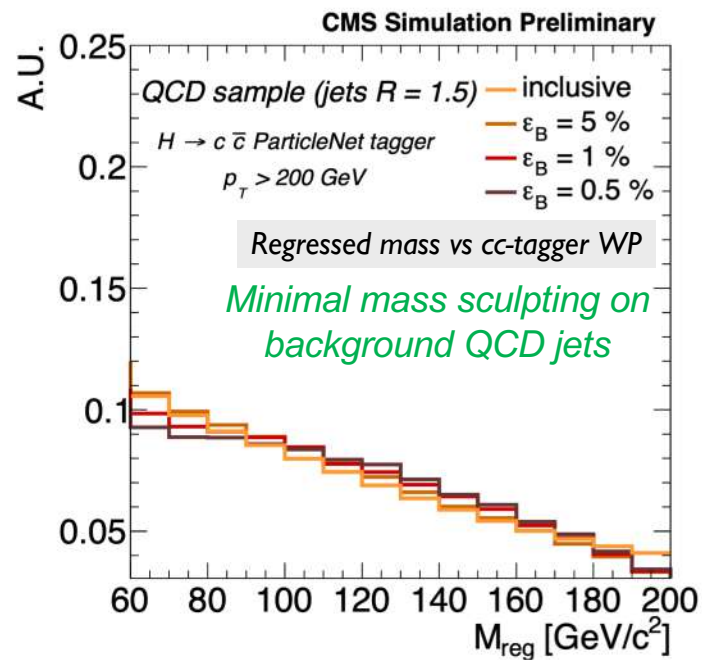
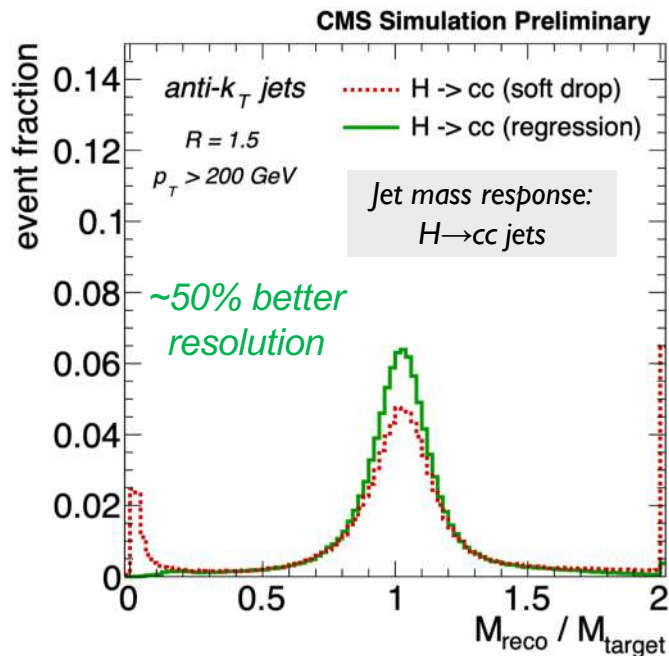
- ❑ Need to measure ParticleNet cc-tagging efficiency in data
 - No pure sample of $H \rightarrow cc$ jets (or even $Z \rightarrow cc$) in data
 - Using $g \rightarrow cc$ in QCD multi-jet events as a proxy
- ❑ Difficulty: select a phase-space in $g \rightarrow cc$ that resembles $H \rightarrow cc$
 - Solution: BDT developed to distinguish hard 2-prong splittings from soft cc
 - Adjust the similarity between proxy and signal jets via BDT cuts
- ❑ Fit to the secondary vertex mass in the “passing” and “failing” regions simultaneously to extract the scale factors (typically 0.9—1.3)
 - three templates: cc (+ single c), bb (+ single b), light flavor jets
 - corresponding uncertainties are 20—30%



Large-R jet mass regression

- ❑ Jet mass: one of the most powerful observable to distinguish signal and backgrounds
- ❑ New ParticleNet-based regression algorithm to improve the large-R jet mass reconstruction

[CMS DP-2021/017](#)



**20 – 25% improvement
in the final sensitivity**

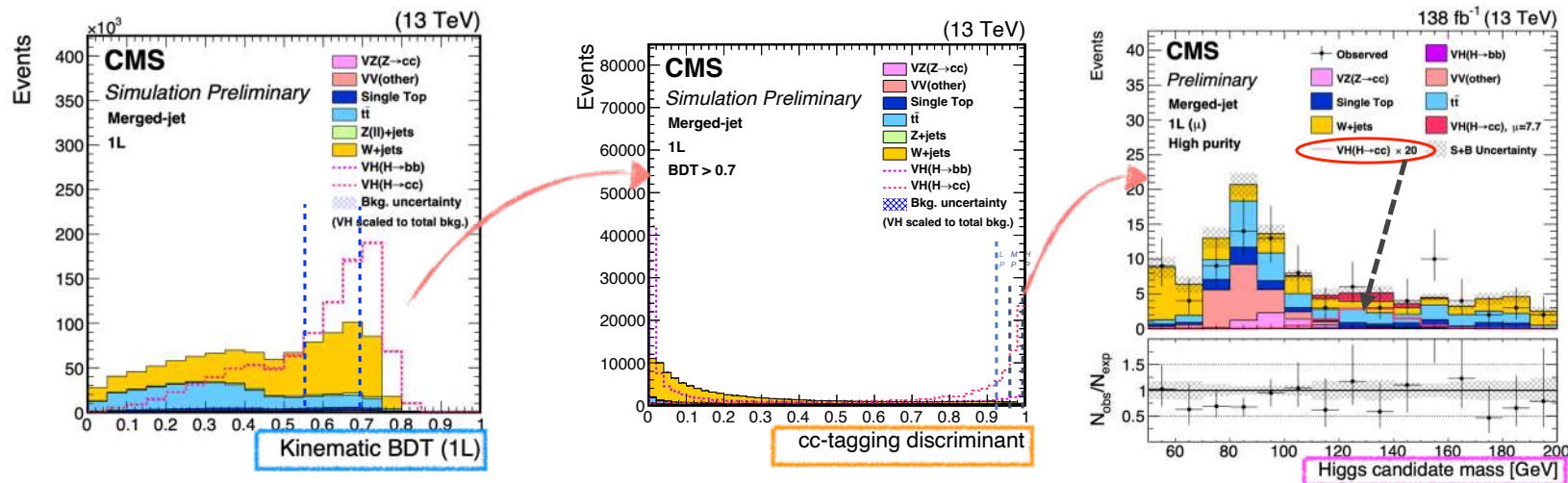
Analysis strategy – merged-jet topology

Factorized approach for analysis design

- event-level kinematic BDT developed in each channel to better suppress main backgrounds (V+jets, tt)
 - using only *event kinematics*, no intrinsic properties (e.g., mass/flavor) of the large-R jet
- ParticleNet cc-tagger then used to define 3 cc-flavor enriched regions and reject light/bb-flavor jets
- finally: fit to the ParticleNet-regressed large-R jet mass shape for signal extraction

Kinematic BDT, ParticleNet cc-tagger and regressed jet mass largely independent of each other

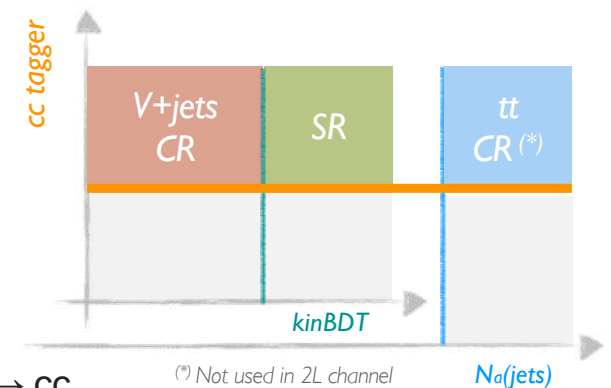
- Sand robust strategy for background estimation and signal extraction



Background estimation

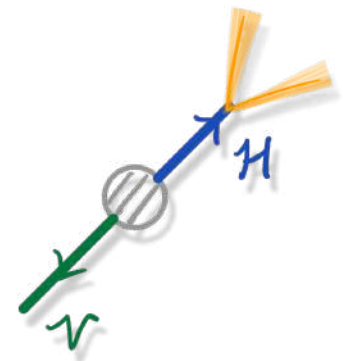
- Normalizations of main backgrounds estimated via dedicated data control regions (CRs)
 - V+jets CR: use the low kinematic BDT region
 - tt CR (0L & 1L): invert the cut on the number of additional small-R jets (i.e., $N_{aj} \geq 2$)
 - free-floating parameters scale the normalizations in CRs and signal regions (SRs) simultaneously

- CRs designed to have similar jet flavor composition as the SR
 - flavor-independent kinematic BDT + same cc-tagging requirement in CRs as in SR
 - allows to correct cc-tagging efficiency for backgrounds directly from data
 - cc-tagging SFs only needed for the signal $VH(H \rightarrow cc)$ process (and $VZ(Z \rightarrow cc)$)
 - conservative uncertainty (2x/0.5x) for the misidentification of $H(Z) \rightarrow bb$ as $H(Z) \rightarrow cc$

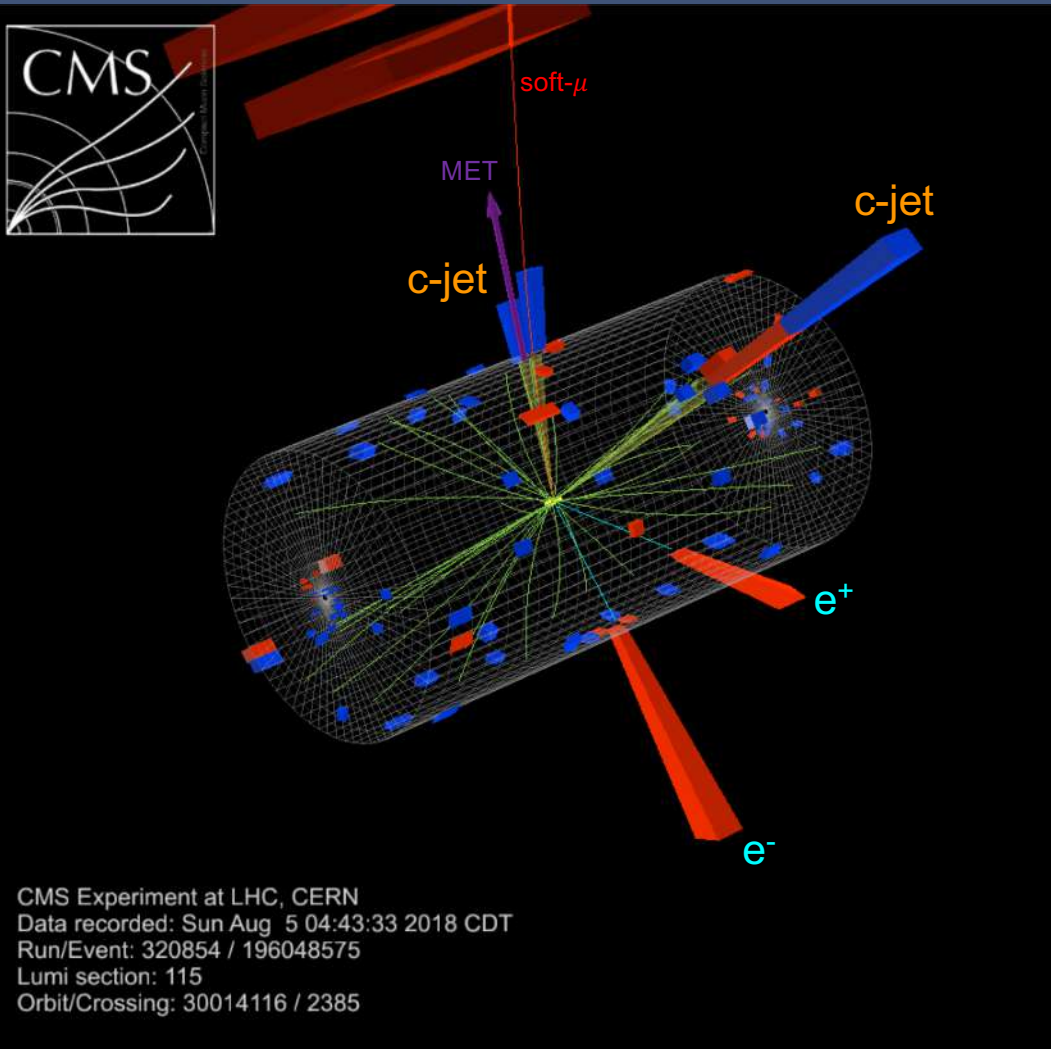


- Minor backgrounds (single top, dibosons, $VH(H \rightarrow bb)$) estimated from simulation
 - dibosons: applying differential NNLO QCD + NLO EW corrections as a function of $p_T(V)$ [[JHEP 2002 \(2020\) 087](#)]

Resolved-jet topology



Overview of the resolved-jet topology



□ Higgs candidate reconstruction

- Select two AK4-jets with the highest c-tagger discriminant score as Higgs jets
- Dedicated c-jet energy regression for improved c-jet energy scale and resolution (eg. recovery of neutrino, unclustered hadrons, etc.) + Recover FSR-jets
- Kinematic-fit (2L channels)

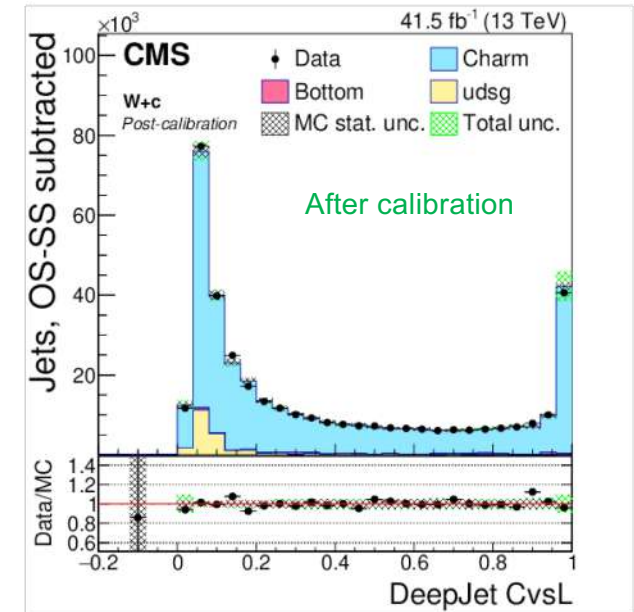
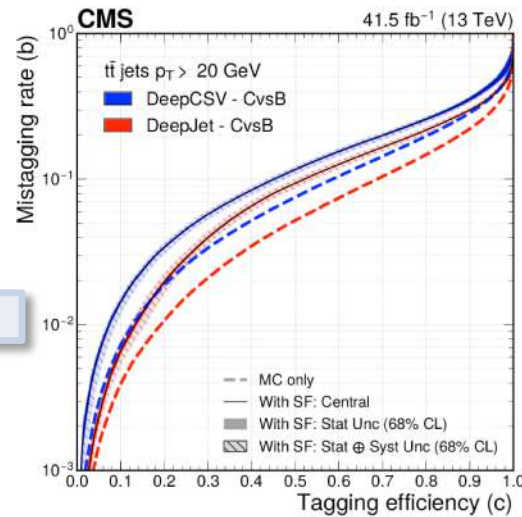
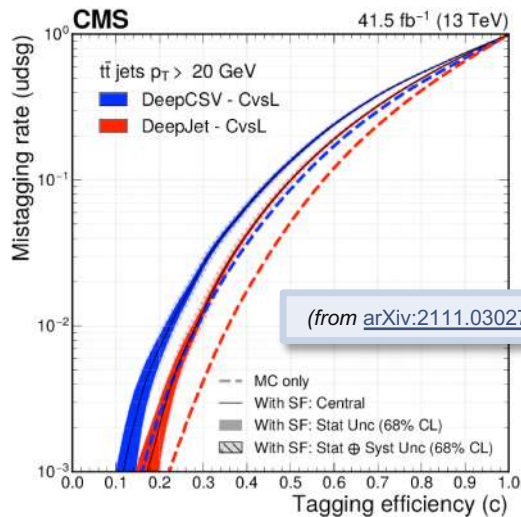
□ Analysis strategy (three channels: 0L, 1L, 2L)

- Control regions for background normalizations
- BDT for final signal extraction

Charm-tagging in the resolved-jet topology

DeepJet algorithm as charm tagger

- ❑ C-jets have “intermediate” properties to b- and light-jets
 - Separate **c-jets** simultaneously from **light-jets** and **bottom jets**
- ❑ From DeepJet output score it is possible to build two c-jet taggers
 - CvsL: it is optimized to differentiate charm-jets from light- or gluon-jets
 - CvsB: it is optimized to differentiate charm-jets from bottom-jets

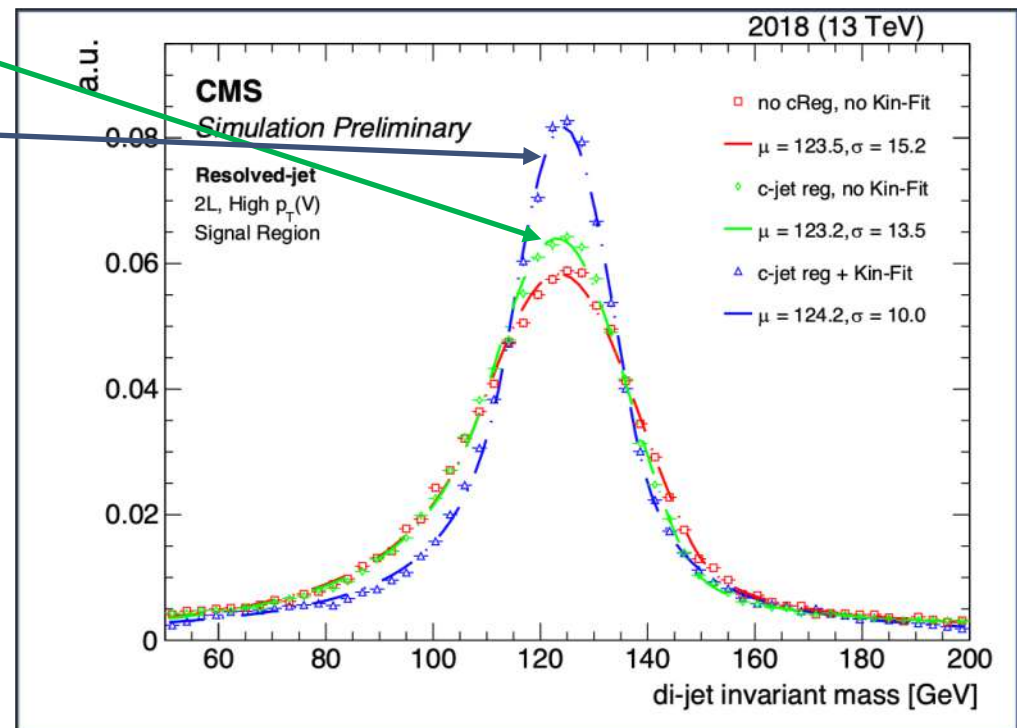
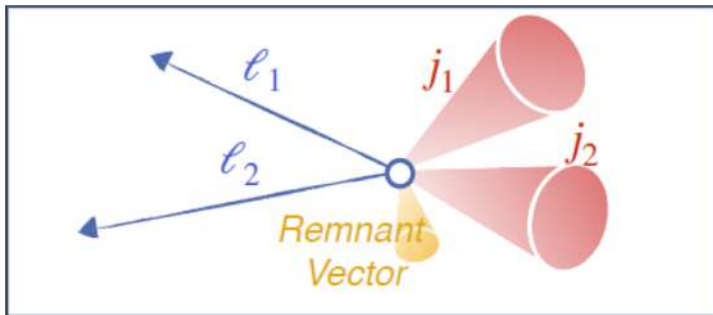


- ❑ Calibration in data with a novel technique!
- ❑ [2022 JINST 17 P03014](#) (published by JINST)
- ❑ Improvement vs DeepCSV (used in 2016 analysis)
 - Increase leading-jet c-tagging efficiency by ~30% for fixed b-jet and light-jet mis-tagging rate

Improvement of the di-jet invariant mass reconstruction

- Dedicated c-jet energy regression + FSR-jet recovery
 - Up to ~15% improvement in Higgs mass resolution

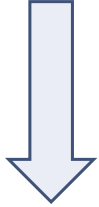
- kinematic fit in the 2L channel:
 - Constrain di-lepton system to the Z boson mass
 - Balance the $\ell\ell+cc+jets$ system in the (p_x, p_y) plane
 - Allow MET to adjust within the experimental resolution



- Up to ~30% improvement in Higgs mass resolution

Analysis categories and background estimation

- Accurate modeling of jet flavor in V+Jet background is vital for proper signal extraction



- Selections optimized for the different decay of the vector boson considered

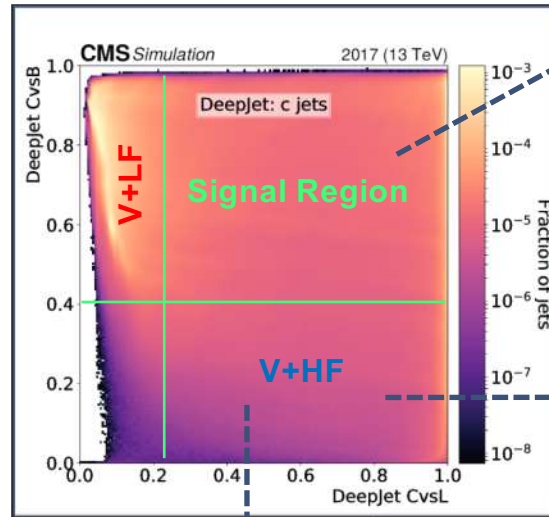
- Definition of 4 analysis categories

- 0L:** $p_T(Z) > 170$ GeV
- 1L:** $p_T(W) > 100$ GeV
- 2L Low- p_T :** $60 \text{ GeV} < p_T(Z) < 150$ GeV
- 2L High- p_T :** $p_T(Z) > 150$ GeV

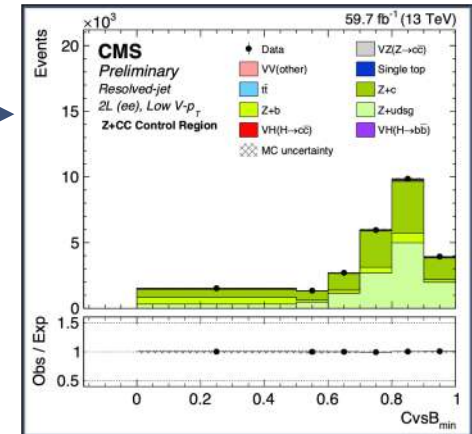
- All the categories have TT, LF, HF and CC CRs (1L has not HF) + 1 SR

- Simultaneous fit to BDT in SR and tagger shapes in CRs

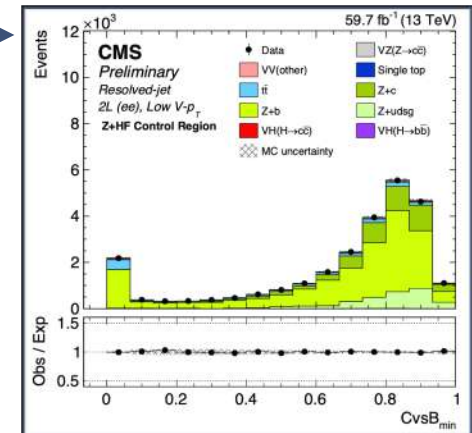
- Separate rate parameters for V+c, V+b, and V+light processes (no W+b) + $t\bar{t}$ + jets
- Freely floating in each channel/year



V+CC
(\bar{c})
Veto $m(H)$
region



$t\bar{t}$
(\bar{c})
Invert Z mass (2L)
Require add jet (1L)*
Require add ℓ and jets (0L)



*1L: also require MET < 170 GeV to keep orthogonal to 0L $t\bar{t}$ CR

The image features a decorative graphic on the left side, composed of several overlapping geometric shapes. At the top is a light blue trapezoidal shape that tapers to the right. Below it is a dark blue trapezoidal shape, also tapering to the right, which overlaps the bottom edge of the light blue shape. At the bottom left, there is a thin, light blue horizontal bar that overlaps the bottom edge of the dark blue shape. The word "Results" is written in white, bold, sans-serif font on the dark blue background.

Results

Uncertainties

- All correlated between topologies, except:
 - Background normalization SFs for V+jets and $t\bar{t}$
 - c-tagging efficiencies
- Main uncertainties
 - Limited statistics of data
 - Statistical uncertainties of V+jets samples
 - Charm tagging efficiencies

Uncertainty source	$\Delta\mu / (\Delta\mu)_{\text{tot}}$
Statistical	85%
Background normalizations	37%
Experimental	48%
Sizes of the simulated samples	37%
Charm identification efficiencies	23%
Jet energy scale and resolution	15%
Simulation modeling	11%
Luminosity	6%
Lepton identification efficiencies	4%
Theory	22%
Backgrounds	17%
Signal	15%

VZ(Z→cc) results

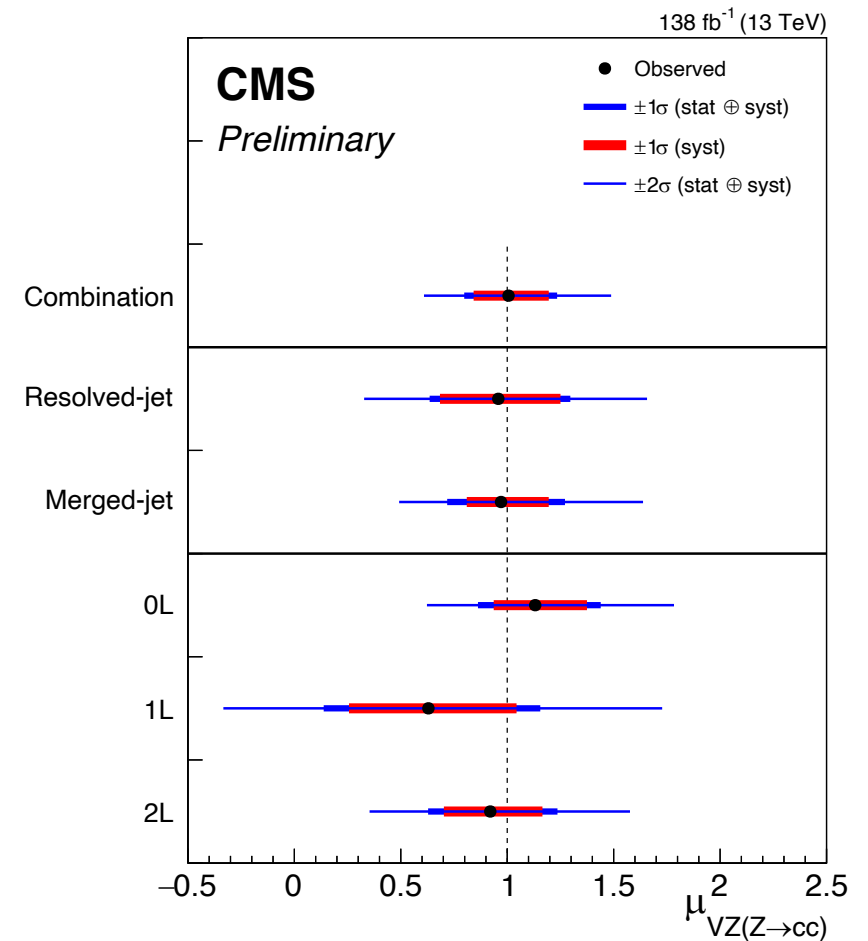
- Analysis validated by looking for VZ(Z→cc) process
 - Same analysis procedure, but extracting VZ(Z→cc) signal
 - Resolved-jet: retrained BDTs with VZ(Z→cc) as signal
 - VH(H→cc) fixed to SM expectation

- Observed (expected) signal strength for VZ(Z→cc):

$$\mu_{VZ(Z\rightarrow cc)} = 1.01_{-0.21}^{+0.23} (1.00_{-0.20}^{+0.22})$$

with a significance of 5.7σ (5.9σ)

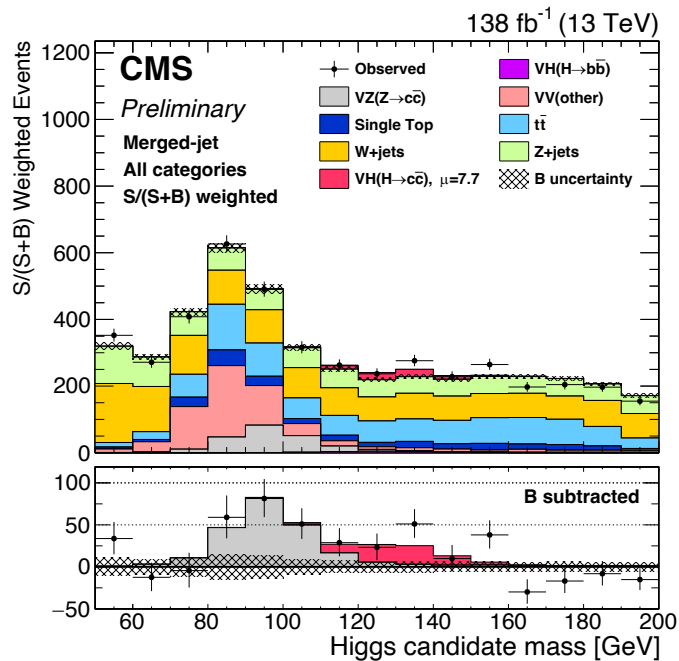
- First observation of Z→cc at hadron collider!**



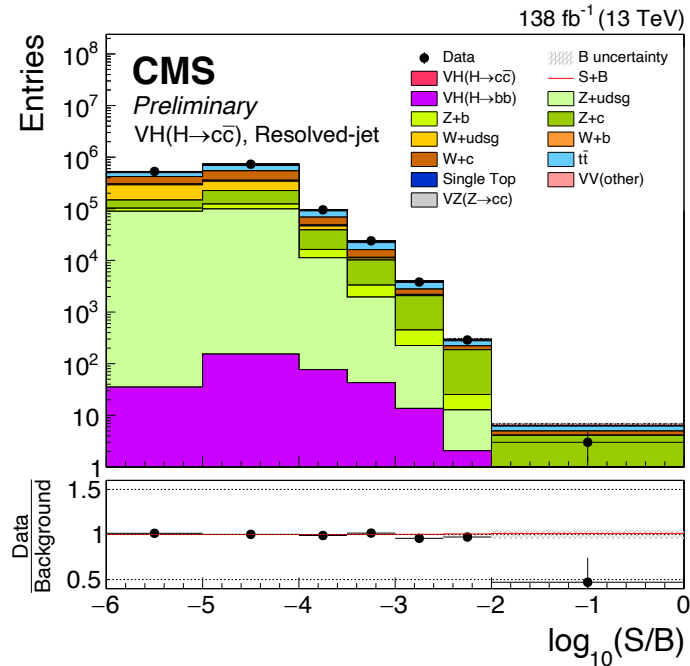
VH(H→cc) results

- ❑ Merged-jet topology: distribution of the Higgs boson candidate mass
- ❑ Resolved-jet topology and the combination: ordering the events by $\log_{10}(S/B)$

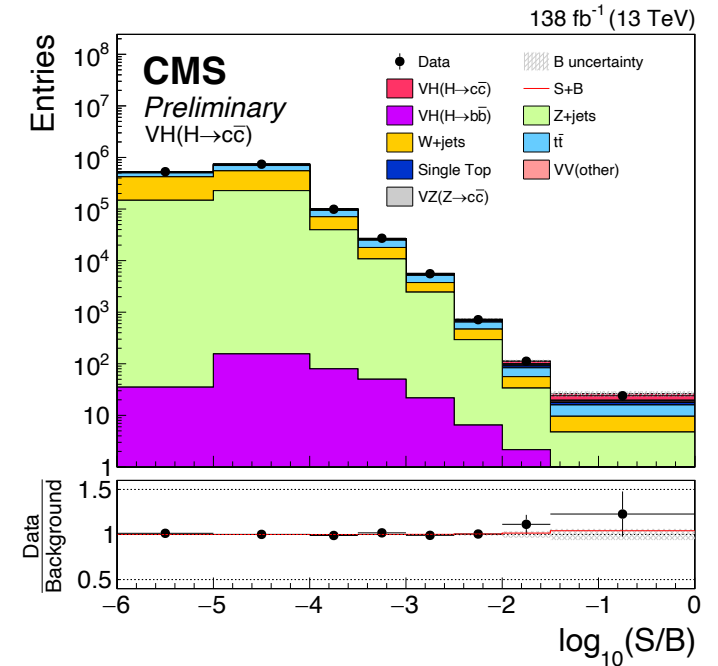
Merged-jet



Resolved-jet



Merged + Resolved



VH(H→cc) results

Observed (expected) upper limit on VH(H→cc) signal strength at 95% CL: $\mu_{VH(H\rightarrow cc)} < 14 (7.6^{+3.4}_{-2.3})$

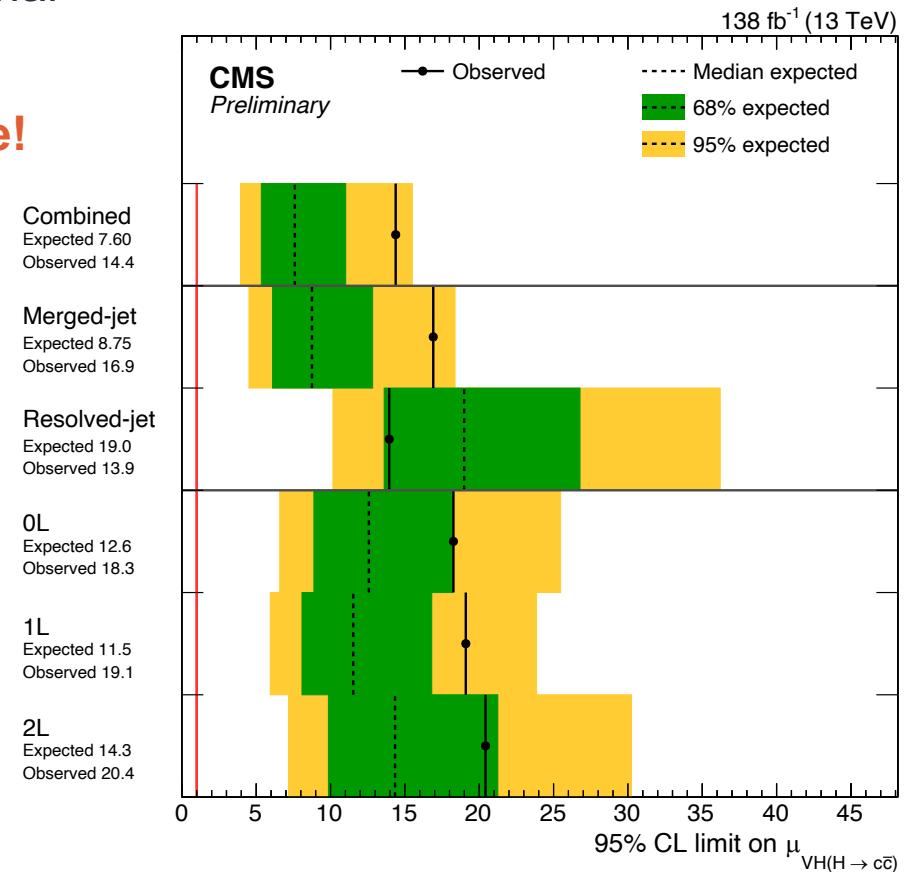
- Strongest limits on VH(H→cc) process to date!
- ATLAS Full Run 2 result: $\mu_{VH(H\rightarrow cc)} < 26 (31)$ [[arXiv:2201.11428](https://arxiv.org/abs/2201.11428)]

Best fit signal strength: $\mu_{VH(H\rightarrow cc)} = 7.7^{+3.8}_{-3.5}$

- Consistent with the SM prediction within 2σ

Obs. (Exp.) upper limits from each topology:

- Resolved-jet topology: **14(19) × SM**
- Merged-jet topology: **17(8.8) × SM**



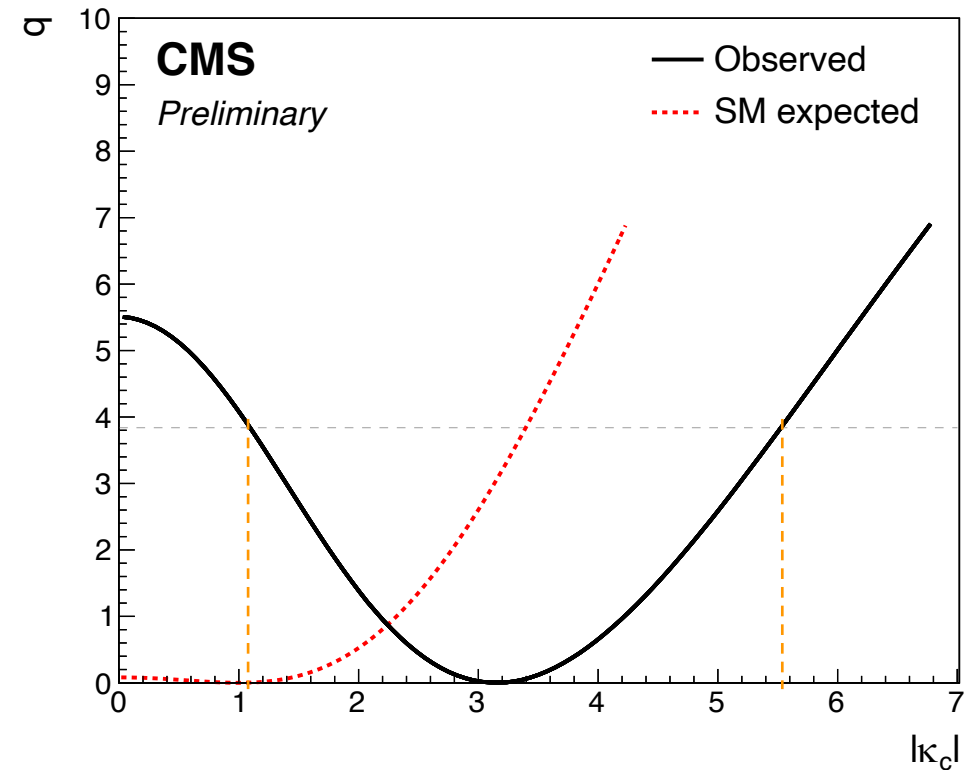
VH(H→cc) results

Results used to place new constraints on κ_c

- Only considering effects on $\mathcal{B}(H \rightarrow cc)$ and fixing all other couplings to their SM values

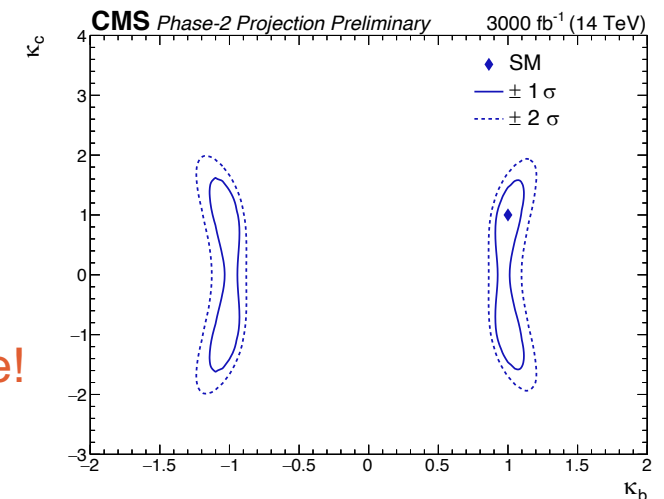
$$\mu_{VH(H \rightarrow cc)} = \frac{\kappa_c^2}{1 + \mathcal{B}_{SM}(H \rightarrow cc) \times (\kappa_c^2 - 1)}$$

- The 95% CL intervals obtained with likelihood scans
 - observed: $1.1 < |\kappa_c| < 5.5$
 - expected: $|\kappa_c| < 3.4$
- **Strongest constraints on $|\kappa_c|$ to date**
 - Competitive with indirect measurements of $|\kappa_c|$: [PRD 92 \(2015\) 033016](#) and [arXiv:2202.00487](#)
 - Comparable to the previous projection for HL-LHC [[ATL-PHYS-PUB-2021-039](#)]



Conclusions

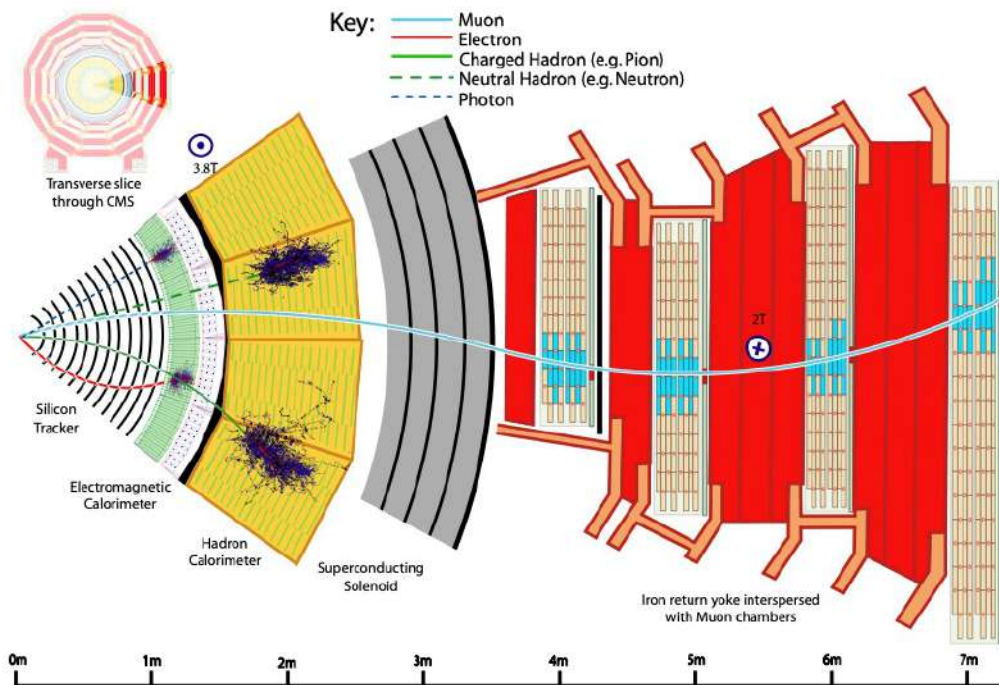
- ❑ New results of the CMS search for the $VH(H \rightarrow cc)$ process are presented
 - Benefit from the full Run 2 dataset
 - Substantial improvements in charm tagging performance
 - Major upgrades of analysis techniques, such as jet energy/mass regression, kinematic fits, etc.
- ❑ Analysis validated by measuring $VZ(Z \rightarrow cc)$ signal strength: $\mu_{VZ(Z \rightarrow cc)} = 1.01^{+0.23}_{-0.21}$
 - Significance of 5.7σ (5.9σ) → First observation of $Z \rightarrow cc$ at a Hadron Collider!
- ❑ Upper limits on $VH(H \rightarrow cc)$: $\mu_{VH(H \rightarrow cc)} < 14$ (7.6 exp.)
 - ~5x increase in exp. sensitivity vs [JHEP 03 \(2020\) 131](#)
 - Constraints on Higgs-charm coupling:
 $1.1 < |\kappa_c| < 5.5$ ($|\kappa_c| < 3.4$ exp.) — Most stringent to date!
- ❑ Projection for HL-LHC: $\mu_{VH(H \rightarrow cc)} < 1.6$ exp.



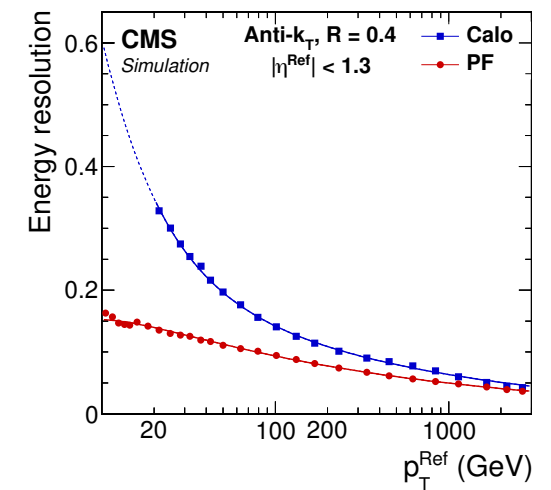
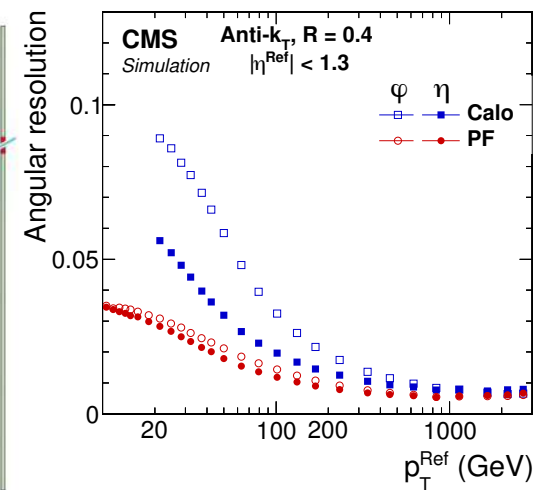
Backups

Particle-flow reconstruction

- Particle-flow (PF): powerful approach for jet reconstruction and flavor tagging
 - excellent energy and angular resolutions
 - each particle (PF candidate) contains a rich set of information from multiple sub-detectors — inputs to deep-learning

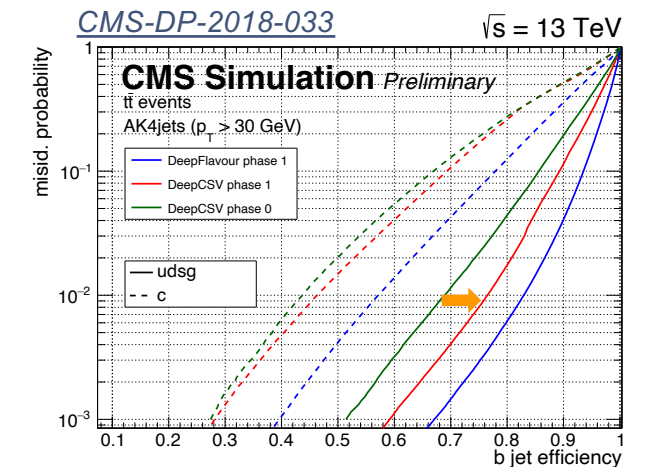
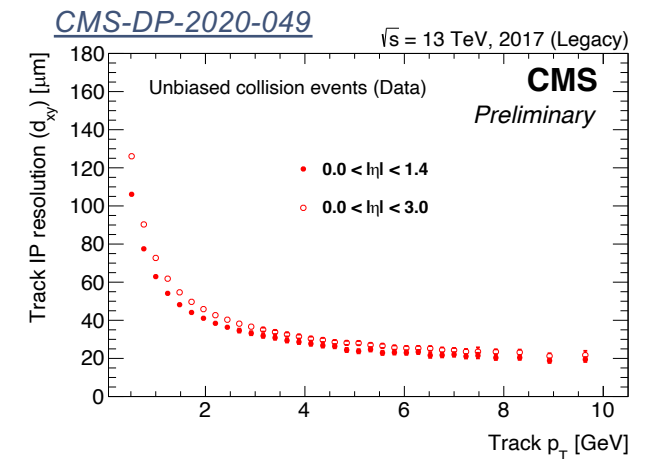
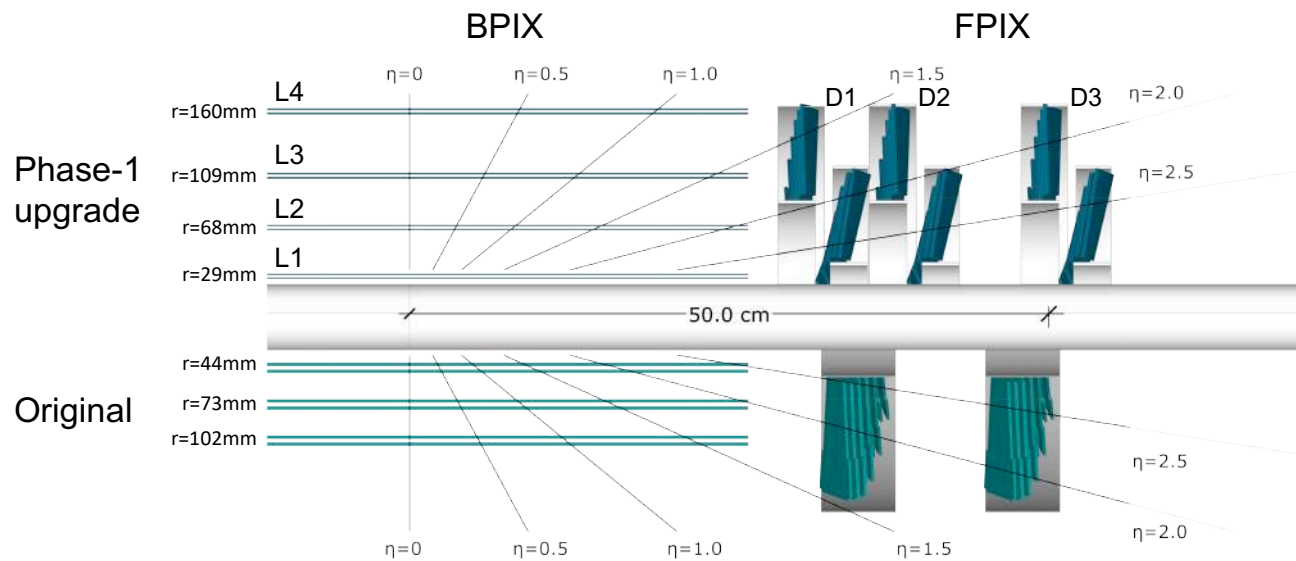


JINST 12 (2017) P10003



Phase-1 pixel detector upgrade

- New pixel detector installed during year-end stop 2016/2017



Improved tracking and flavour tagging performance in the 2017 — 2018 data set!

H \rightarrow cc searches at the LHC

□ ATLAS:

- [[Phys. Rev. Lett. 120 \(2018\) 211802](#)] (36 fb⁻¹)
- [[arXiv:2201.11428](#)] (139 fb⁻¹)
- [[ATL-PHYS-PUB-2021-039](#)] (HL-LHC projection, 3000 fb⁻¹)

□ CMS:

- [[JHEP 03 \(2020\) 131](#)] (36 fb⁻¹)
- [[CMS-PAS-HIG-21-008](#)] (138 fb⁻¹; HL-LHC projection, 3000 fb⁻¹)

□ LHCb:

- [[LHCb-CONF-2016-006](#)] (1.98 fb⁻¹)
- [[LHCb-PUB-2018-009](#)] (HL-LHC projection, 300 fb⁻¹)

Baseline event selections

Merged-jet topology

Variable	0L	1L	2L
p_T^ℓ	—	(>25,>30)	>20
Lepton isolation	—	(<0.06, —)	(<0.25, —)
$N_{a\ell}$	=0	=0	—
$M(\ell\ell)$	—	—	75–105
$N_{\text{small-R}}^{\text{aj}}$	<2	<2	<3
p_T^{miss}	>200	>60	—
$p_T(\text{V})$	>200	>150	>150
$p_T(\text{H}_{\text{cand}})$	>300	>300	>300
$m(\text{H}_{\text{cand}})$	50–200	50–200	50–200
$\Delta\phi(\text{V}, \text{H}_{\text{cand}})$	>2.5	>2.5	>2.5
$\Delta\phi(\vec{p}_T^{\text{miss}}, j)$	>0.5	—	—
$\Delta\phi(\vec{p}_T^{\text{miss}}, \ell)$	—	<1.5	—
Kinematic BDT	>0.55	0.55–0.7, >0.7	>0.55
$c\bar{c}$ discriminant			
High purity	>0.99	>0.99	>0.99
Medium purity	0.96–0.99	0.96–0.99	0.96–0.99
Low purity	0.90–0.96	0.90–0.96	0.90–0.96

Resolved-jet topology

Variable	0L	1L	2L low- $p_T(\text{V})$	2L high- $p_T(\text{V})$
p_T^ℓ	—	(>25,>30)	>20	>20
Lepton isolation	—	(<0.06, —)	(<0.25, —)	(<0.25, —)
$N_{a\ell}$	=0	=0	—	—
$M(\ell\ell)$	—	—	75–105	75–105
$p_T(j_1)$	>60	>25	>20	>20
$p_T(j_2)$	>35	>25	>20	>20
$CvsL(j_1)$	>0.225	>0.225	>0.225	>0.225
$CvsB(j_2)$	>0.4	>0.4	>0.4	>0.4
$N_{\text{small-R}}^{\text{aj}}$	—	<2	—	—
p_T^{miss}	>170	—	—	—
p_T^{miss} significance	—	>4	—	—
$p_T(\text{V})$	>170	>100	60–150	>150
$p_T(\text{H}_{\text{cand}})$	>120	>100	—	—
$m(\text{H}_{\text{cand}})$	<250	<250	<250	<250
$\Delta\phi(\text{V}, \text{H}_{\text{cand}})$	>2.0	>2.5	>2.5	>2.5
$\Delta\phi(\vec{p}_T^{\text{miss}}, j)$	>0.5	—	—	—
$\Delta\phi(\vec{p}_T^{\text{miss}}, \ell)$	—	<2.0	—	—

Uncertainties

□ Breakdown of the uncertainties in each topology

Merged-jet topology

Table 3: The relative contributions to the total uncertainty on $\mu_{\text{VH}(H \rightarrow c\bar{c})}$ in the merged-jet analysis, with a best fit value $\mu_{\text{VH}(H \rightarrow c\bar{c})} = 8.7^{+4.6}_{-4.0}$.

Uncertainty source	$\Delta\mu / (\Delta\mu)_{\text{tot}}$
Statistical	88%
Background normalizations	39%
Experimental	40%
Sizes of the simulated samples	24%
Charm identification efficiencies	26%
Jet energy scale and resolution	15%
Simulation modeling	1%
Luminosity	5%
Lepton identification efficiencies	2%
Theory	25%
Backgrounds	21%
Signal	14%

Resolved-jet topology

Table 4: The relative contributions to the total uncertainty on $\mu_{\text{VH}(H \rightarrow c\bar{c})}$ in the resolved-jet analysis, with a best fit value $\mu_{\text{VH}(H \rightarrow c\bar{c})} = -9.5 \pm 9.6$.

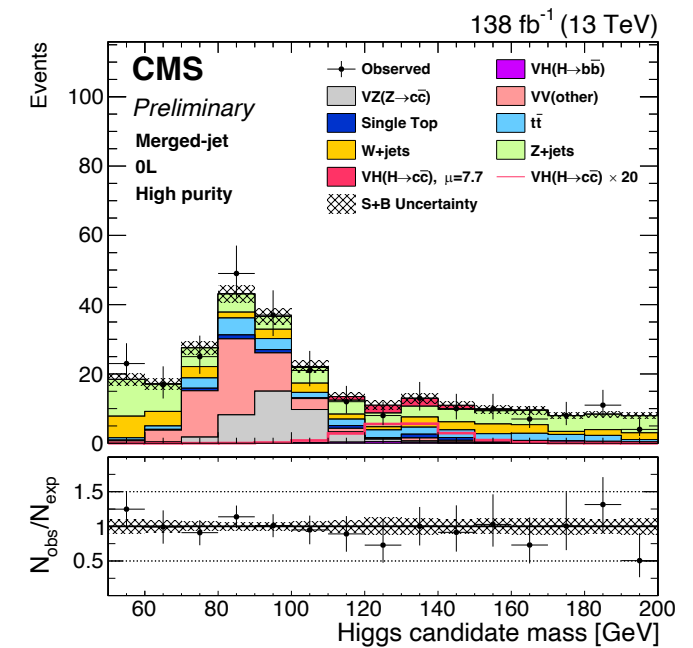
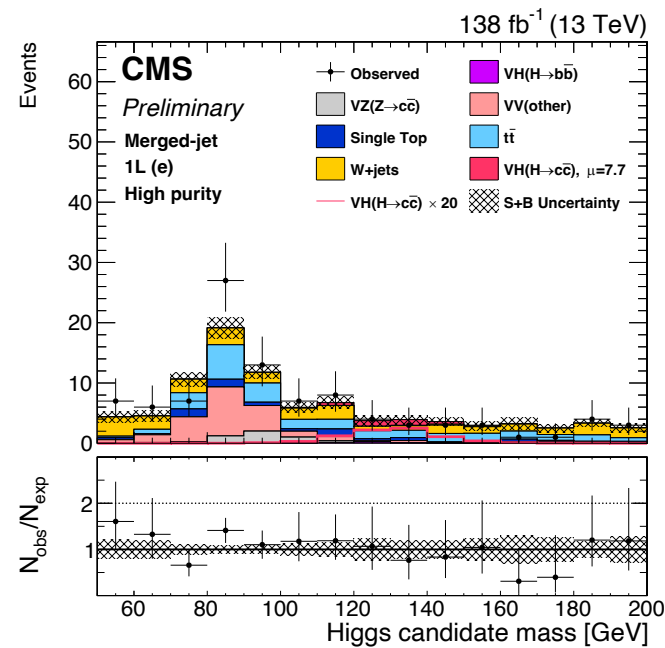
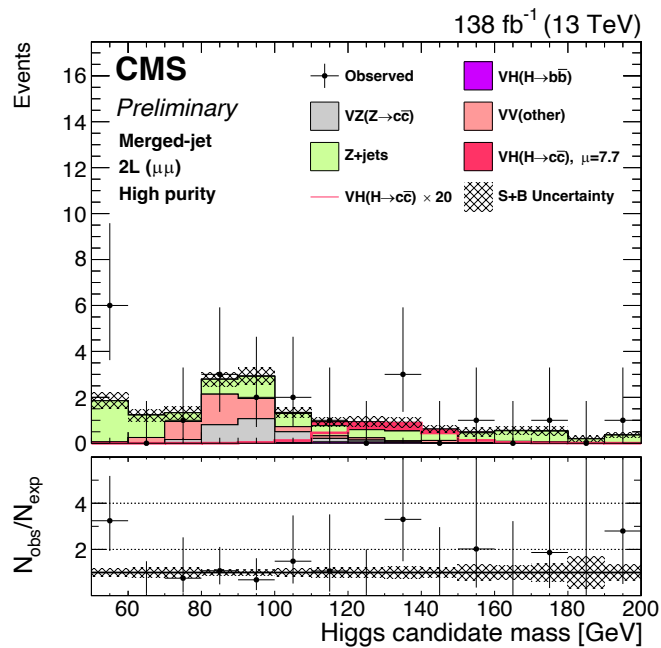
Uncertainty source	$\Delta\mu / (\Delta\mu)_{\text{tot}}$
Statistical	66%
Background normalizations	28%
Experimental	72%
Sizes of the simulated samples	59%
Charm identification efficiencies	27%
Jet energy scale and resolution	17%
Simulation modeling	20%
Luminosity	13%
Lepton identification efficiencies	10%
Theory	22%
Backgrounds	21%
Signal	7%

Merged-jet topology: signal regions

2L($\mu\mu$), high cc-purity

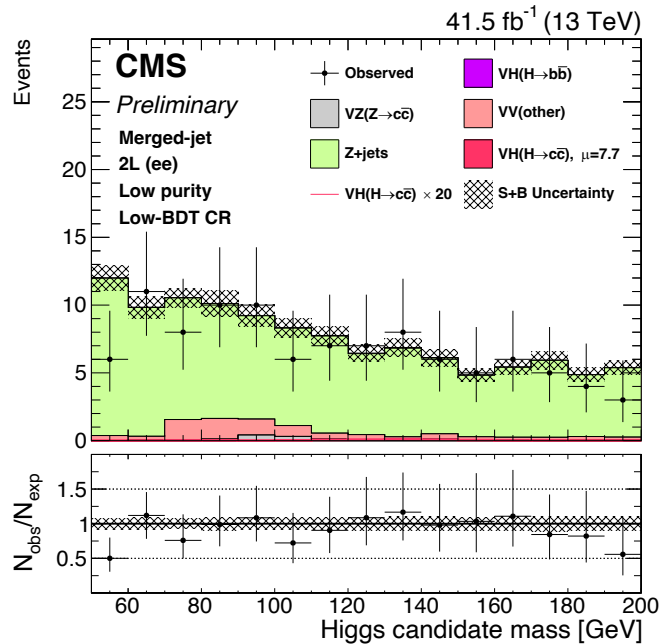
1L(e), high cc-purity

0L, high cc-purity

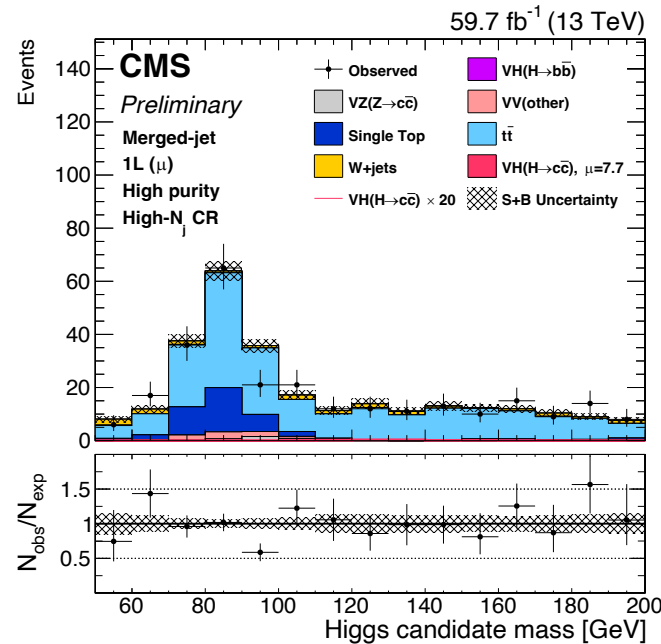


Merged-jet topology: control regions

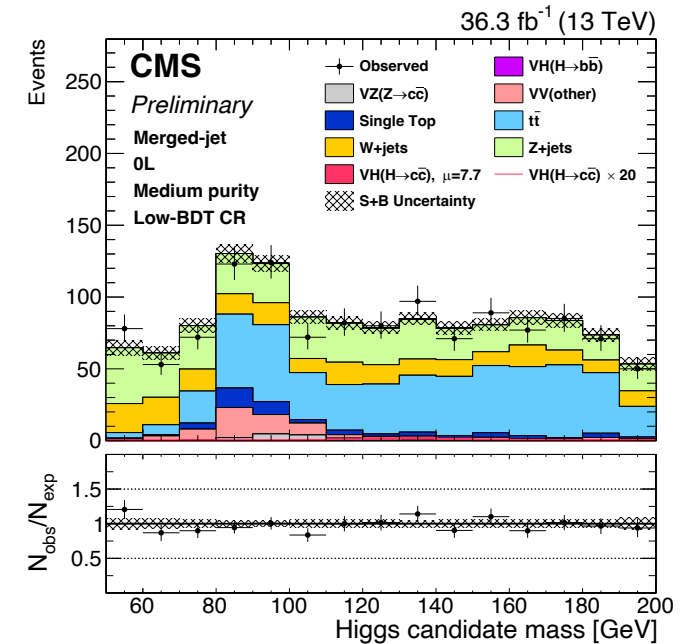
2L(ee), V+jets CR, low cc-purity



1L(μ), tt CR, high cc-purity



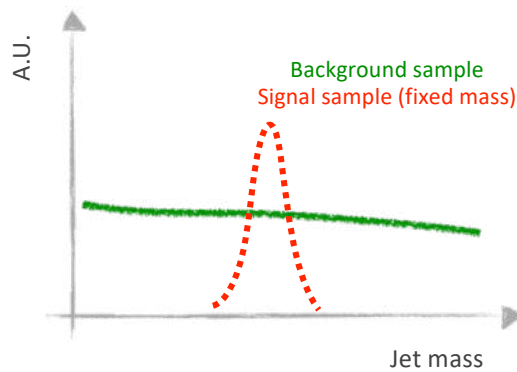
0L, V+jets CR, medium cc-purity



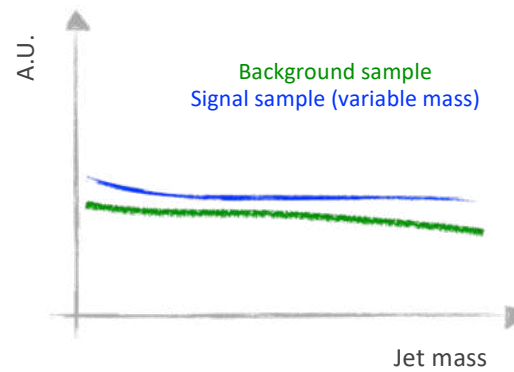
Mass decorrelation

CMS-DP-2020-002

Plain training:
no mass decorrelation



Mass-decorrelated
training



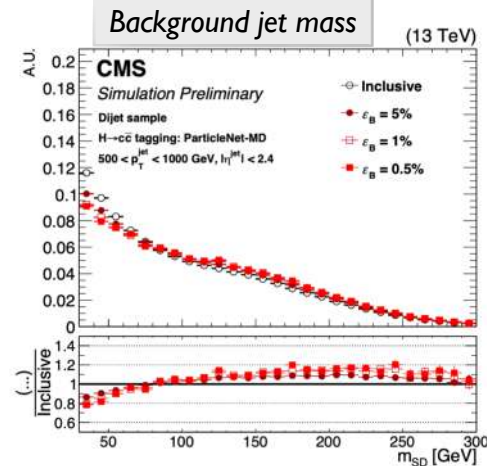
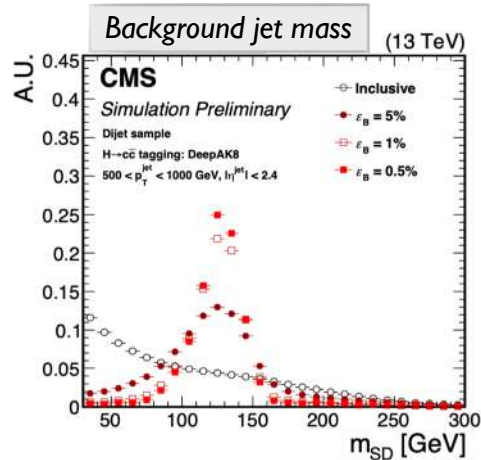
□ “Mass sculpting”: background jet mass shape becomes similar to signal after tagger selection

□ New approach to prevent mass sculpting

- using a special signal sample for training
 - hadronic decays of a spin-0 particle X
 - $X \rightarrow bb$, $X \rightarrow cc$, $X \rightarrow qq$
 - not a fixed mass, but a **flat mass spectrum**
 - $m(X) \in [15, 250]$ GeV

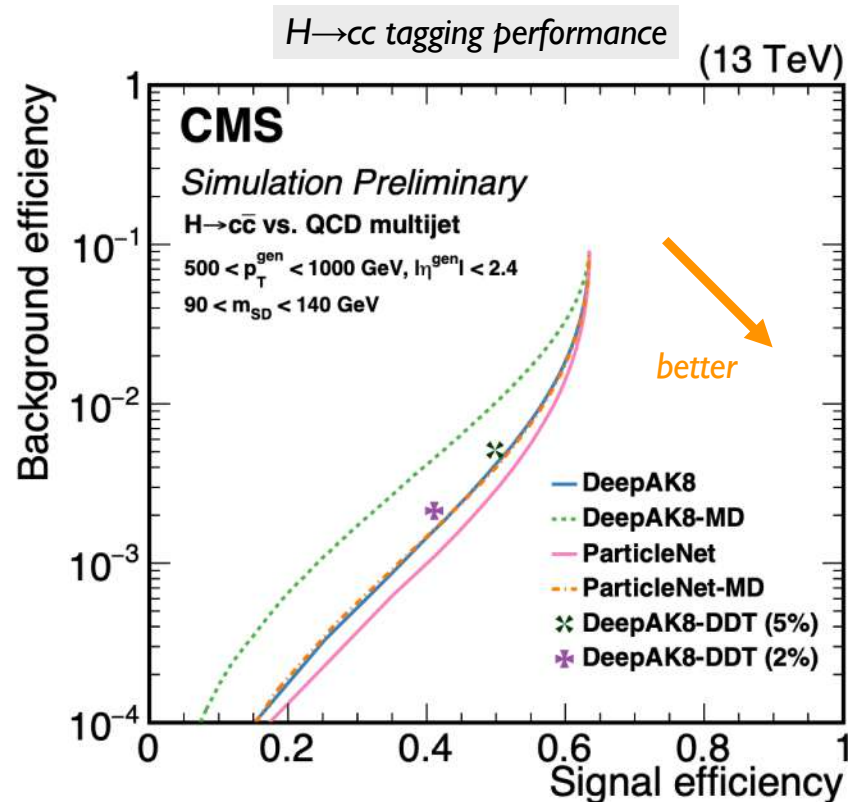
■ allows to easily reweight both signal and background to a \sim flat 2D distribution in (p_T, mass) for the training

□ Signal and background have the same (\sim flat) mass spectrum, thus no sculpting will develop in the training



Mass decorrelation (II)

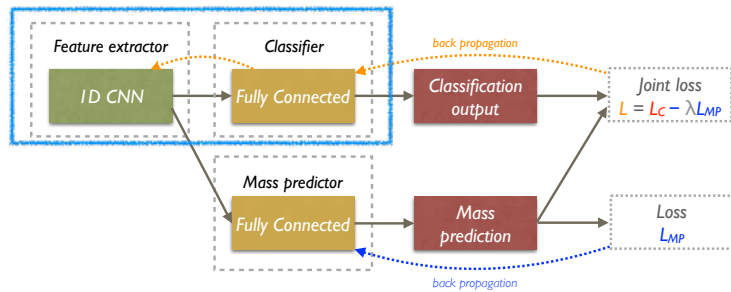
[CMS-DP-2020-002](#)



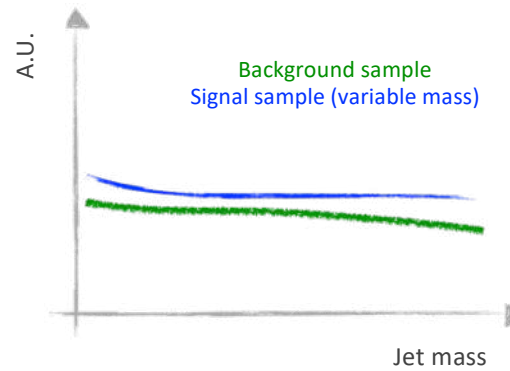
- ❑ “Mass sculpting”: background jet mass shape becomes similar to signal after tagger selection
- ❑ New approach to prevent mass sculpting
 - using a special signal sample for training
 - hadronic decays of a spin-0 particle X
 - X \rightarrow bb, X \rightarrow cc, X \rightarrow qq
 - not a fixed mass, but a **flat mass spectrum**
 - m(X) \in [15, 250] GeV
 - allows to easily reweight both signal and background to a \sim flat 2D distribution in (p_T, mass) for the training
- ❑ Performance loss due to mass decorrelation greatly reduced compared to the previous approach (DeepAK8-MD, based on “adversarial training”)

Comparison of mass decorrelation methods

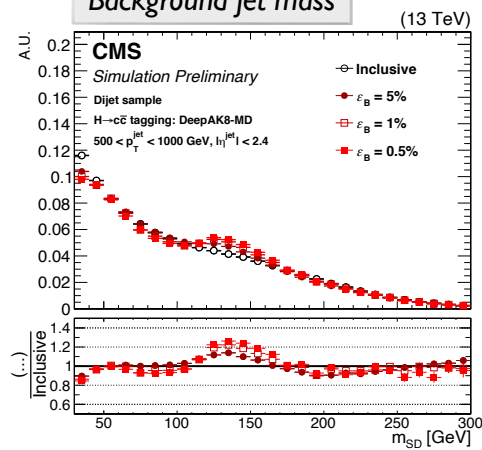
DeepAK8-MD



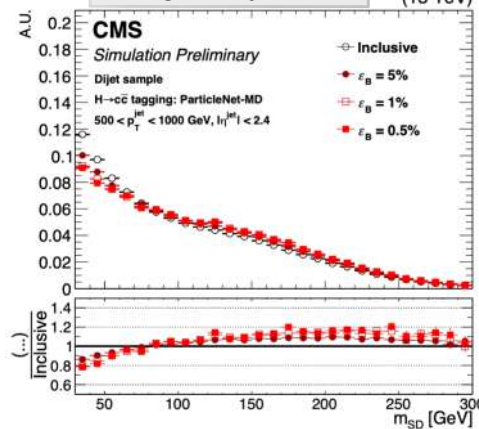
ParticleNet-MD



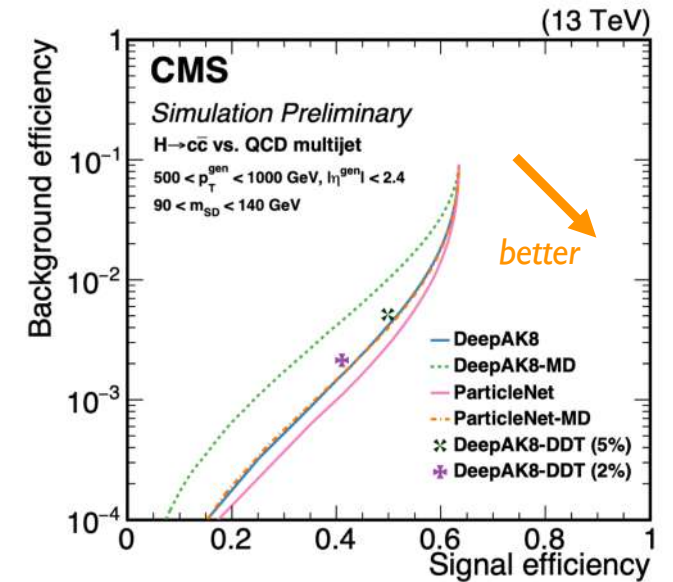
Background jet mass



Background jet mass



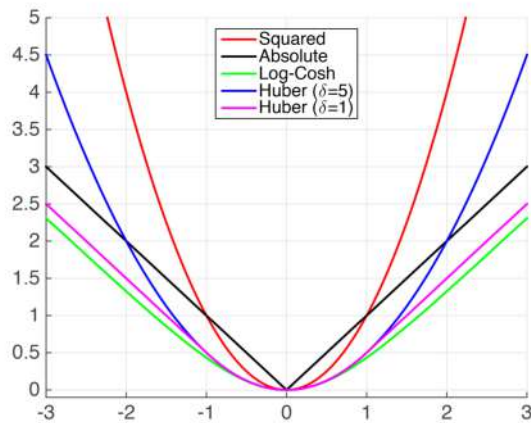
$H \rightarrow c\bar{c}$ tagging performance



Large-R jet mass regression

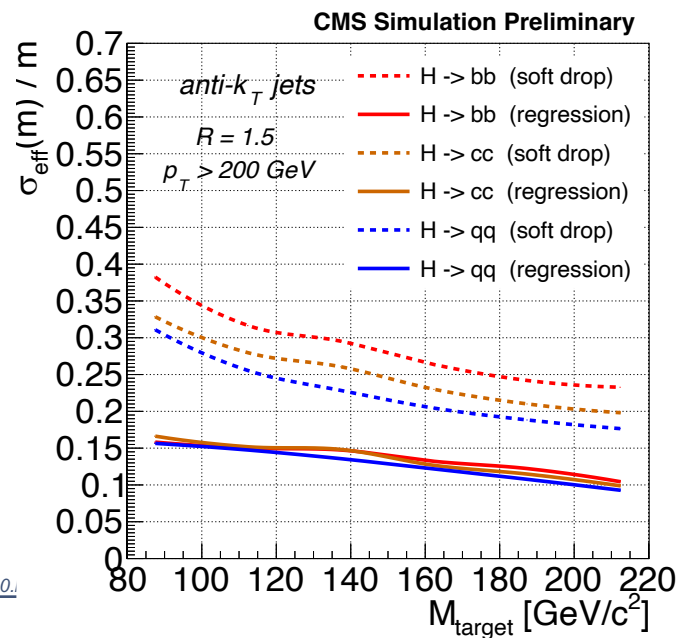
Loss function: LogCosh

$$L(y, y^p) = \sum_{i=1}^n \log(\cosh(y_i^p - y_i))$$

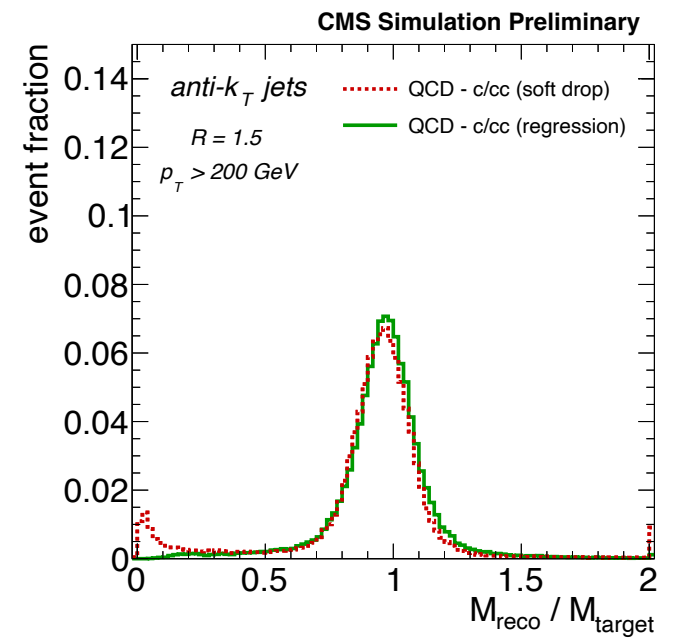


<https://www.cs.cornell.edu/courses/cs4780/2015fa/web/lecturenotes/lecturenote10.>

Signal jet mass resolution



Background jet mass response

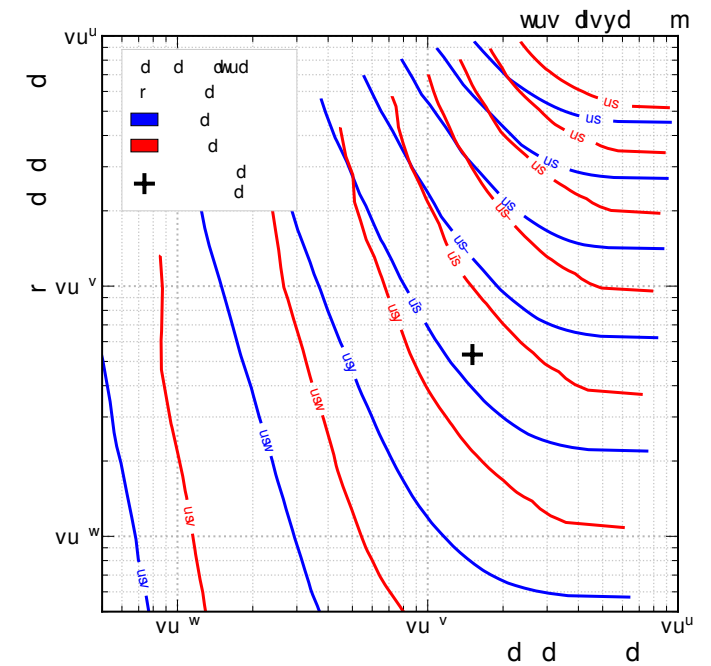
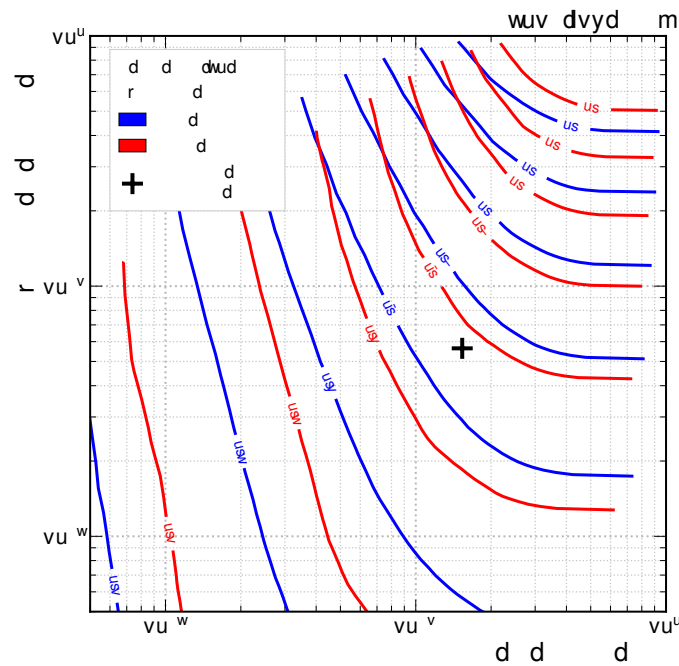
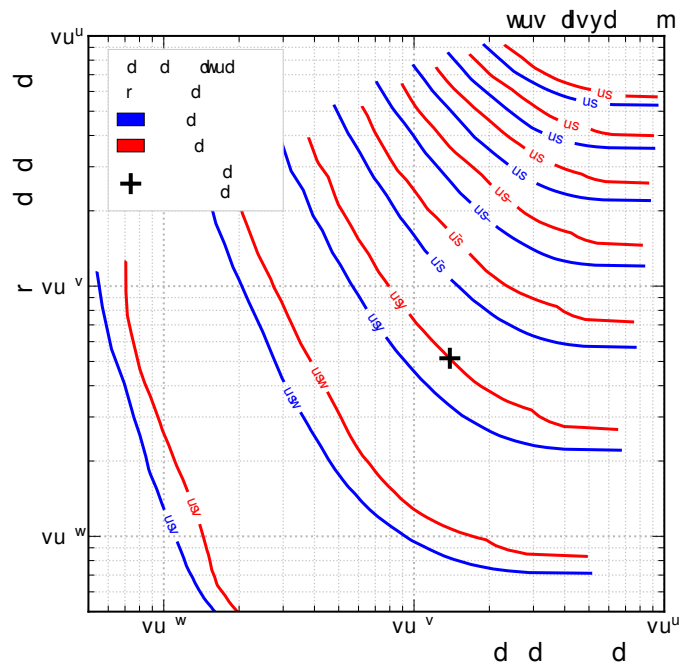


C-tagger ROC curves

2016

2017

2018

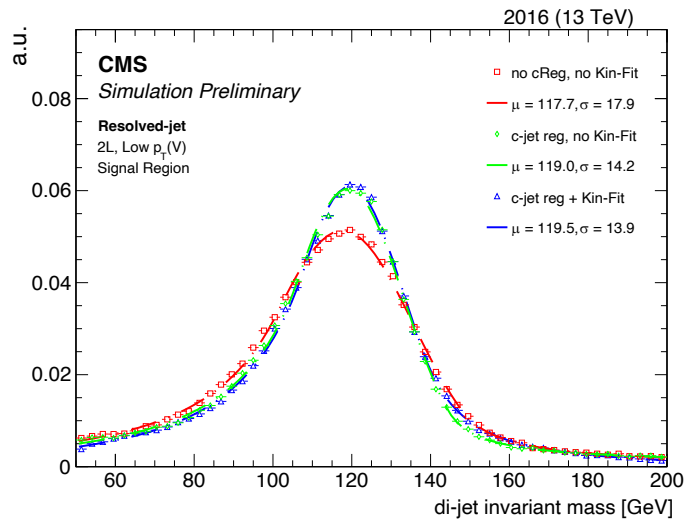


- CMS c-tagging WP: ~40% (c), ~16% (b), ~4% (light)
- ATLAS c-tagging WP [\[arXiv:2201.11428\]](https://arxiv.org/abs/2201.11428): 27% (c), 8% (b), 1.6% (light)

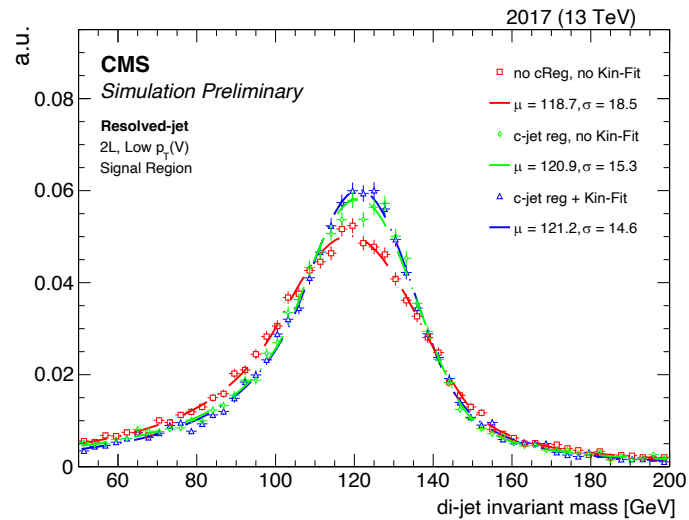
C-jet energy regression and kinematic fit

□ 2-lepton Low- $p_T(V)$ category – $60 \text{ GeV} < p_T(V) < 150 \text{ GeV}$

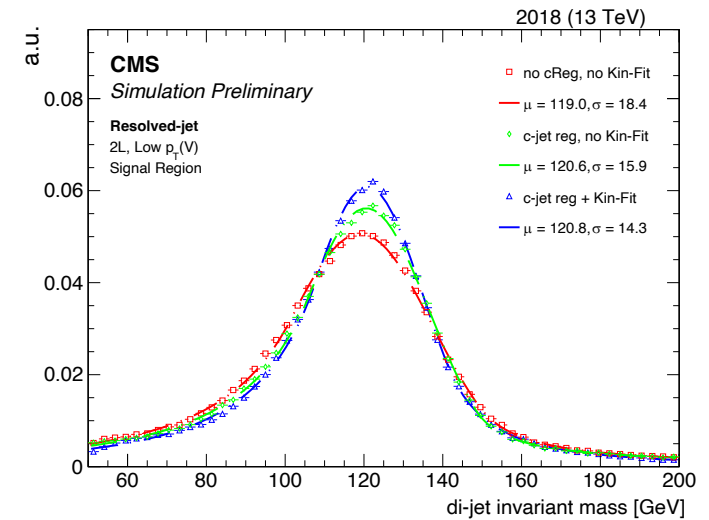
2016



2017



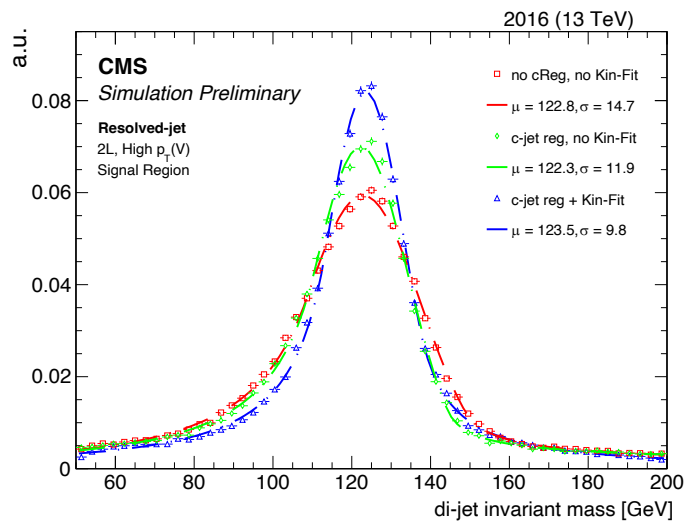
2018



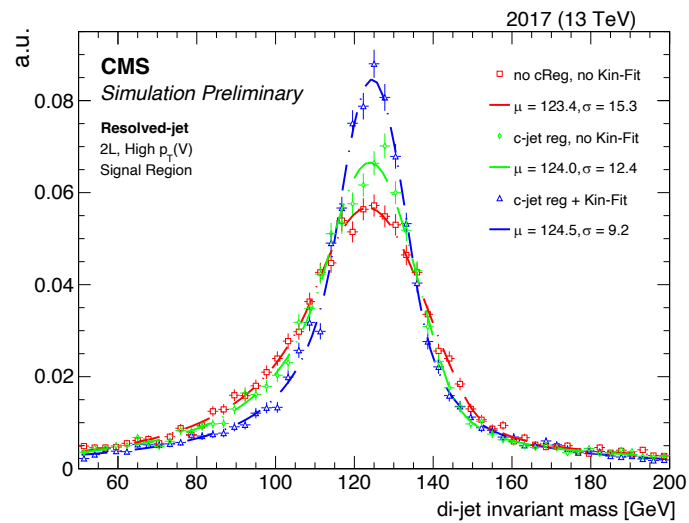
C-jet energy regression and kinematic fit

□ 2-lepton High- $p_T(V)$ category – $p_T(V) > 150$ GeV

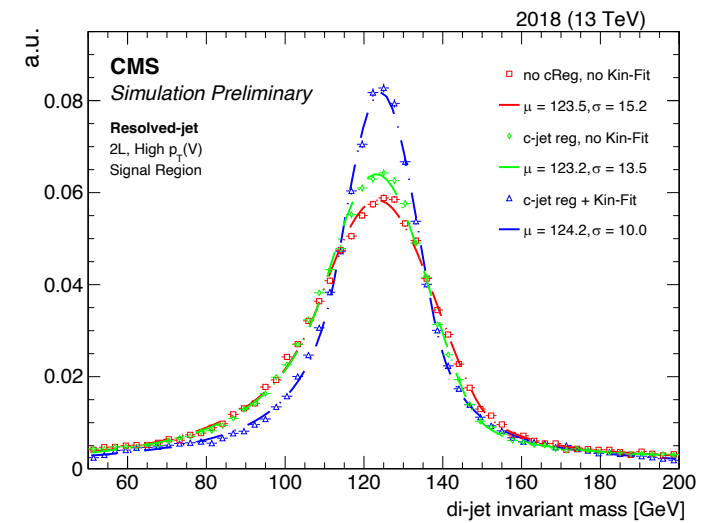
2016



2017



2018



Charm-tagging in the “resolved-jet” topology

DeepJet algorithm – the cornerstone of the VH(cc) resolved-jet topology analysis

❑ Multiclassifier Deep Neural Network

- Optimized for AK4-jets
- Returns the probability for a given jet to be originated by a b-, c- or light-quark

❑ DNN architecture:

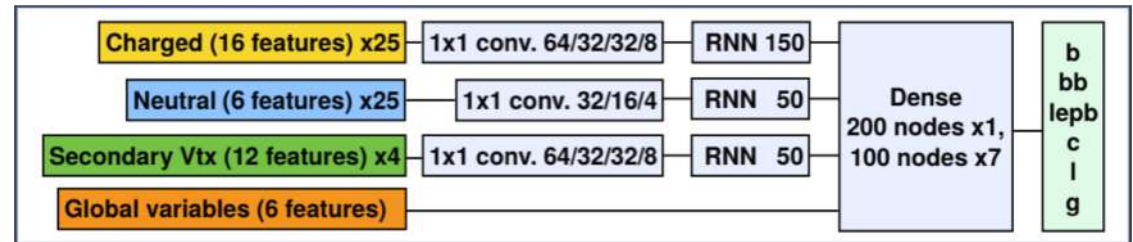
- Separate 1D CNNs to process three low-level feature classes
 - For each class, concatenate multiple CNNs with decreasing dimensions
 - Compress the features to lower dimensional space
- RNNs (LSTM type) applied after CNNs
 - Better handles the variable length sequence (PF candidates/SV)
- Fully connected layer to connect all channels

❑ Input variables:

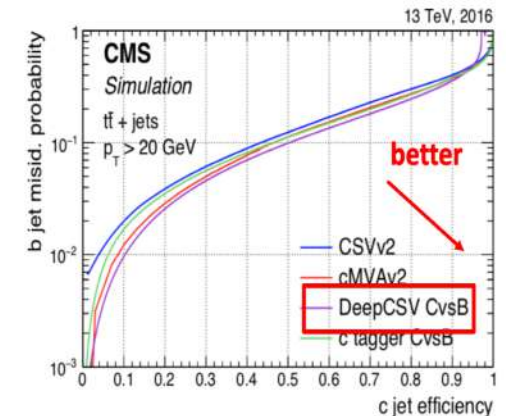
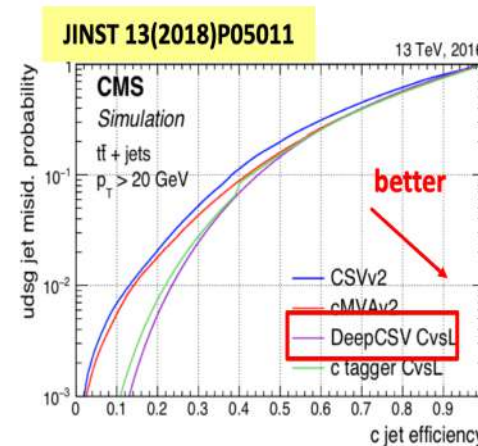
- Properties of PF-candidates
- Global jet features
- Secondary vertices

❑ Output:

- 6 raw scores



DeepJet architecture
(from [2008.10519](#))



- DeepCSV: predecessor of DeepJet
- Used in the CMS VH(cc) analysis with 2016 data [[JHEP 2020,131](#)]

Charm-tagging in the “resolved-jet” topology

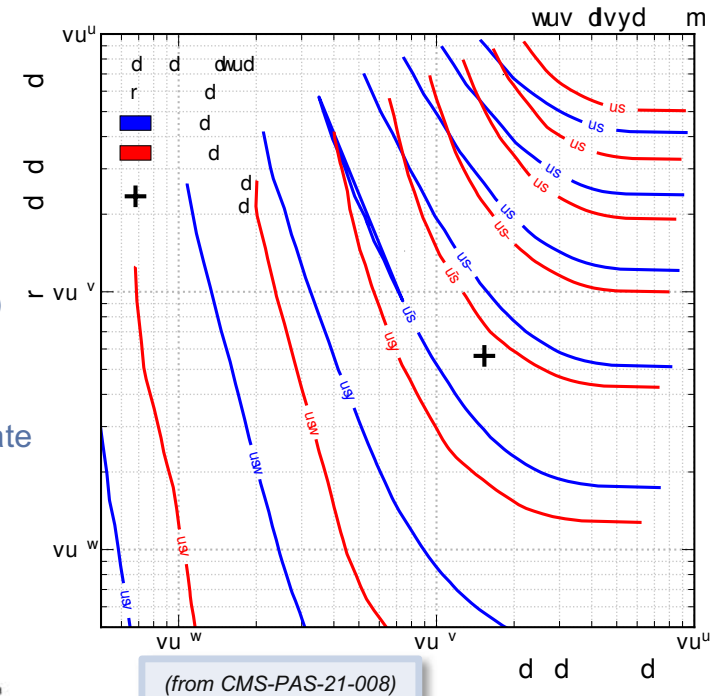
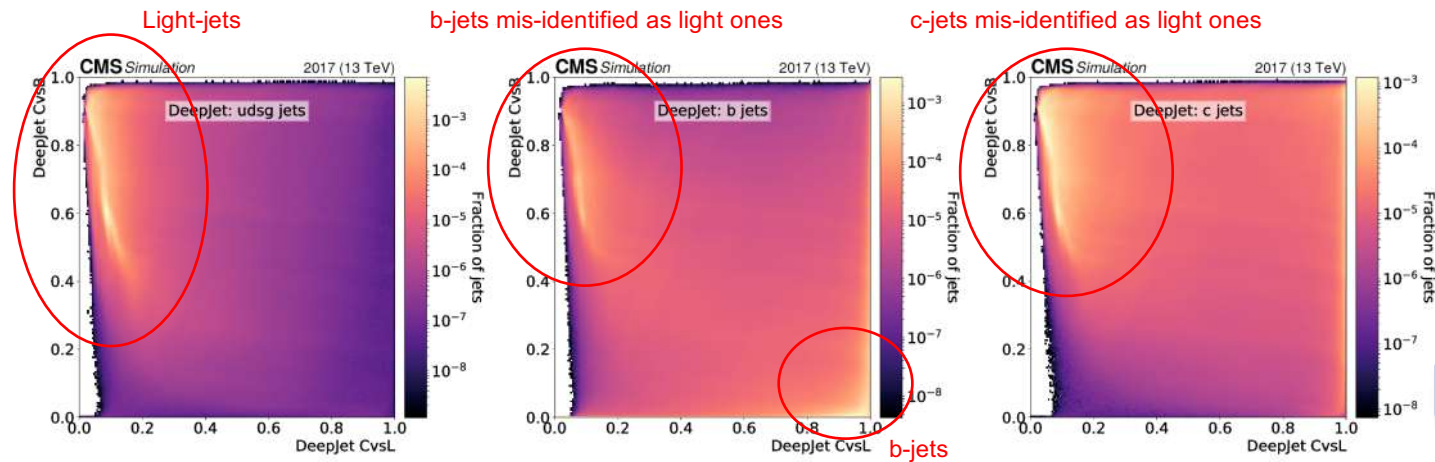
DeepJet algorithm as charm tagger

Definition of leading-jet working point

- Dedicated studies of the simulated jets distribution in the CvsB/CvsL 2D plane
- It's possible to define regions to isolate c-jets vs b- and light-jets
- **CvsL > 0.225, CvsB > 0.4** define the region with c-jet identification efficiency of ~43% with a b-jet and light-jet mis-tagging rate respectively of ~15% and ~4% (depending on the year)

Improvement versus DeepCSV (used in the 2016 VH(cc) analysis)

- Increase leading-jet c-tagging efficiency by ~30% for fixed b-jet and light-jet mis-tagging rate



(from CMS-PAS-21-008)

(from arXiv:2111.03027)

A new method to calibrate charm-taggers

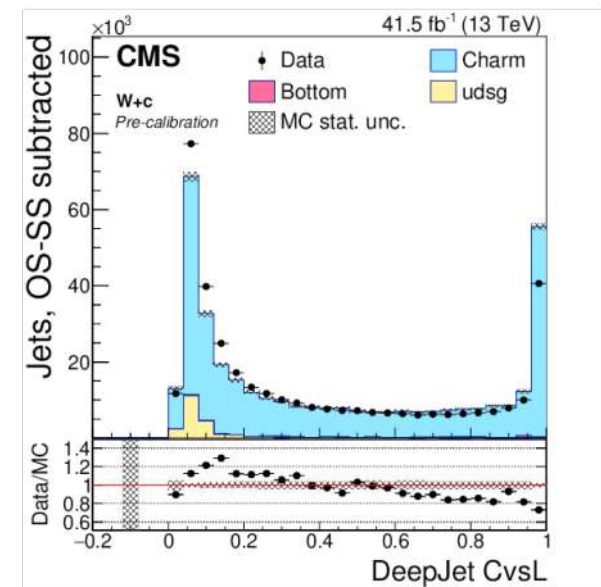
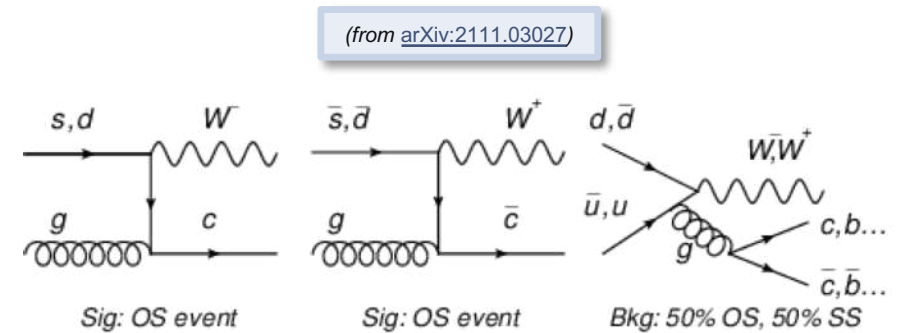
DeepJet algorithm calibration

Methodology

- Iterative approach exploiting three distinct control regions that are enriched with either b-jets, c-jets, or light-flavour and gluon jets
- First time that a calibration method to correct the 2D distribution of c-tagging discriminator shapes is presented → [arXiv:2111.03027](https://arxiv.org/abs/2111.03027) (accepted by JINST)

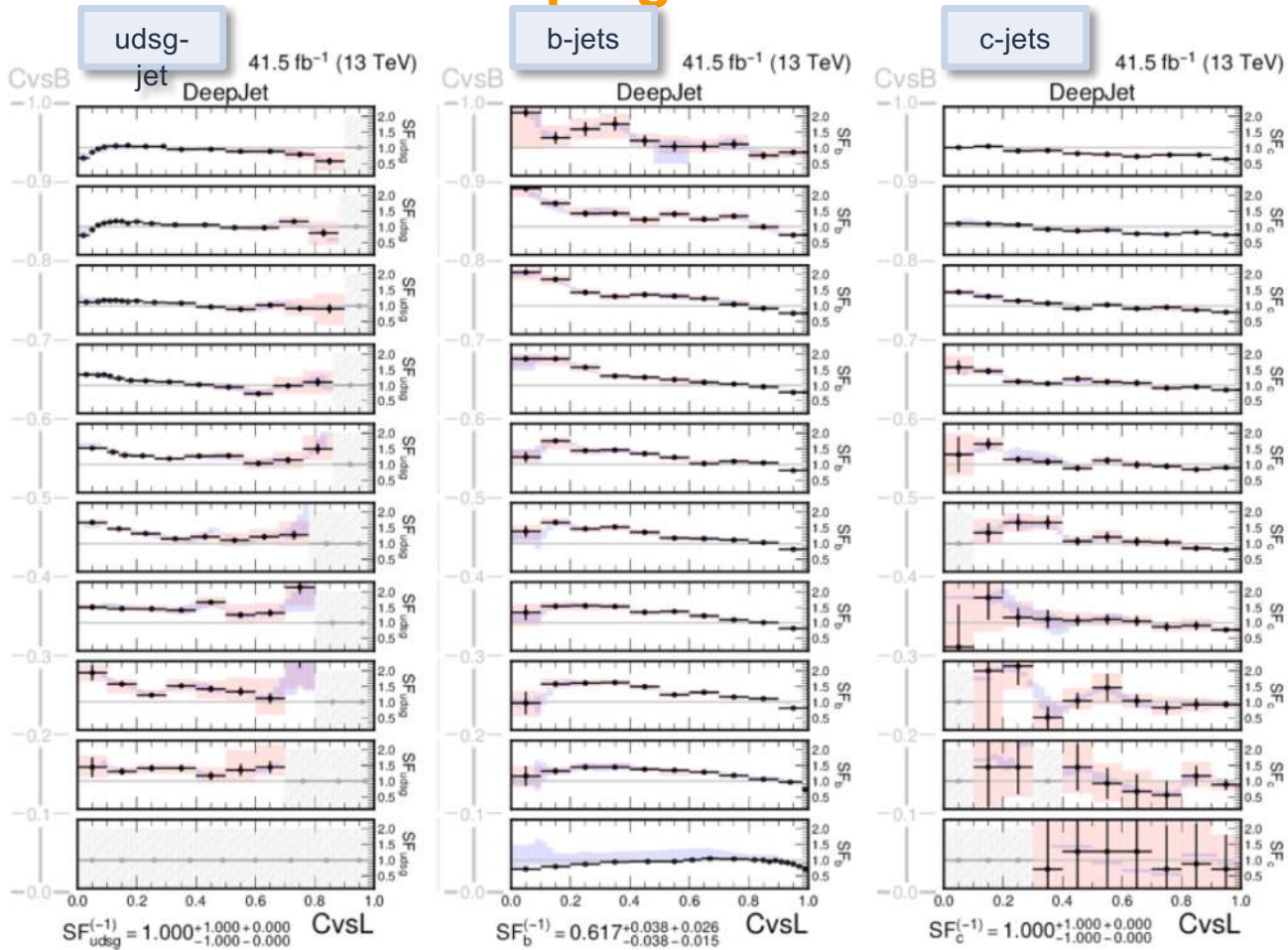
Search for an abundant and pure source of charm-jets

- Target W production in association with charm quarks
 - The relevant events involve a leptonically decaying W boson and a c-jet
 - These c-jets are identified using the semileptonic decay of the charmed hadrons, which produces a soft muon within the jet
- Major background has 50% chance to have SS or OS final states → performing an OS-SS subtraction reduces considerably the W+gluon process
- To enrich in b-jets and light-jets, the semi-(di-)leptonic $t\bar{t}$ +jets and $DY(Z \rightarrow \mu\mu/ee)$ +jets processes are considered



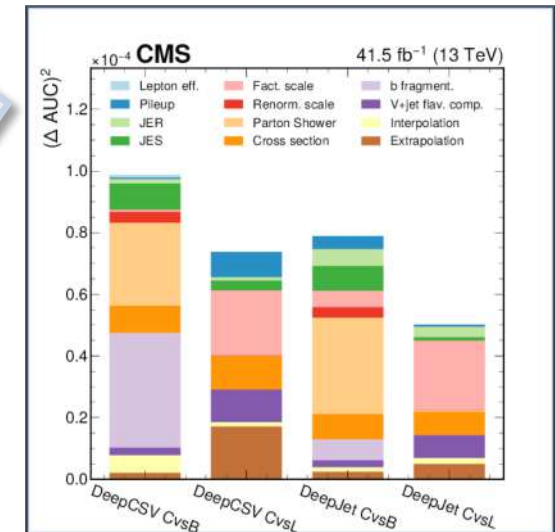
A new method to calibrate charm-taggers

Extraction of reshaping data-to-simulation scale factors



□ SFs as a function of CvsL in bins of CvsB

- Fixed bin width along CvsB and an adaptive binning scheme along CvsL (stat. depending)
- Total uncertainties (red envelopes) relatively small in the region of interest of the analysis
- Total uncertainties breakdown
 - Overall smaller than DeepCSV



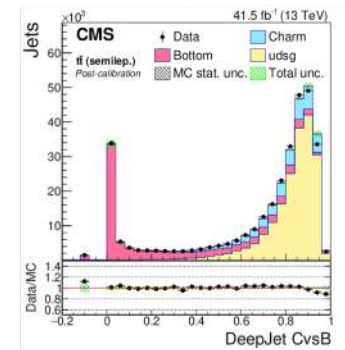
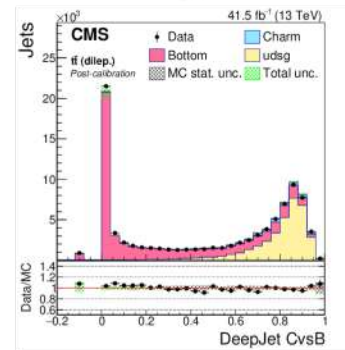
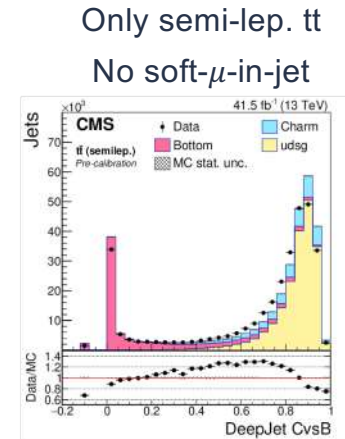
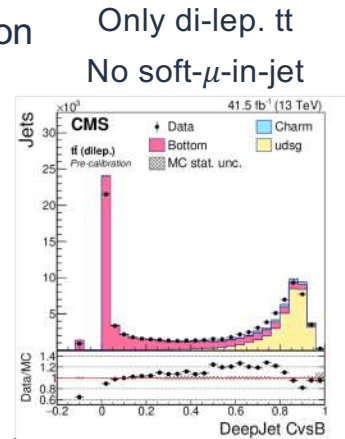
(from arXiv:2111.03027)

A new method to calibrate charm-taggers

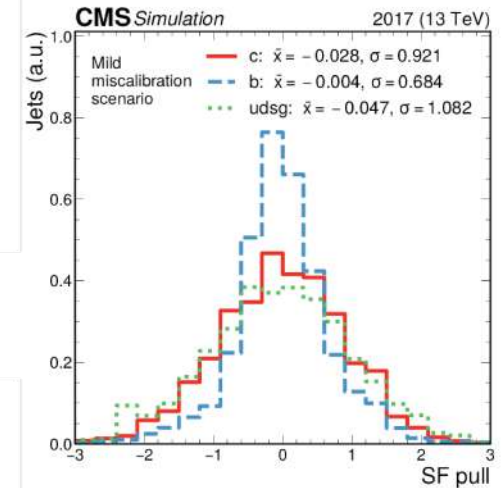
Validate robustness of the SFs derivation

(from arXiv:2111.03027)

- ❑ Check possible bias due to the soft- μ -in-jet selection
 - SFs are derived without soft- μ selection
- ❑ Check possible bias between semileptonic or dileptonic tt final states
 - SFs are derived also for the two separate processes independently
- ❑ Check possible bias due in the fit:
 - Inject *artificial* SFs to calculate the pulls between the fit result and the injected one



Bias test – pull distribution

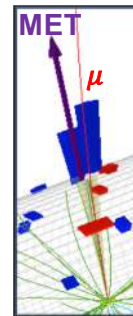


All the checks shown
no bias in the SFs
derivation

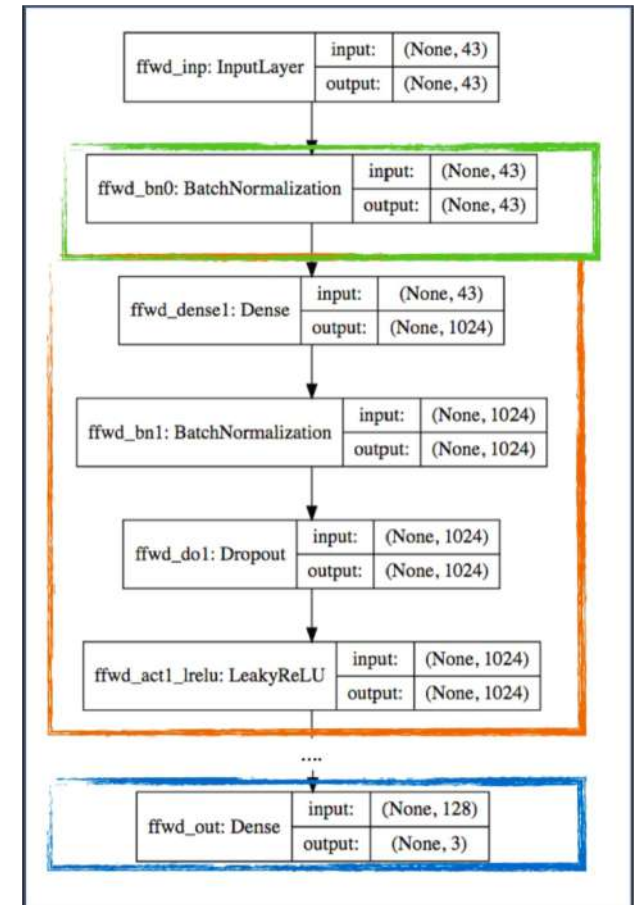
A dedicated charm-jet energy regression

Goal: improve c -jet energy scale and resolution

- ❑ Inspired by b-jet energy regression [[arXiv:1912.06046](https://arxiv.org/abs/1912.06046)]
 - Jet energy measurements not always accurate:
 - loss of neutrinos, hadrons outside jet radius. Effect enhanced in c -jets and b -jets
 - Dedicated algorithm to determine c -jet energy scale and resolution
 - Algorithm pioneered for the observation of the $H \rightarrow b\bar{b}$ decay mode
- ❑ Regression performed using DNN architecture:
 - Feed-forward fully connected Deep NN (neurons with Leaky ReLU activation)
 - 6 hidden layers + batch normalization + dropout
 - Trained using c -jets collected from $W \rightarrow c\bar{q}$ decays in $t\bar{t}$ MC events
 - Target is represented by $p_T(\text{gen})/p_T(\text{reco})$
- ❑ Input features
 - Total of 43 input variables in input to the network
 - Jets: kinematics, energy fraction, leading+soft-lepton tracks, pile-up, secondary vertexes
 - Jet energy shapes (e.g. energy fraction, etc), jet constituents, $p_T(\text{jet})/p_T(\text{lepton})$

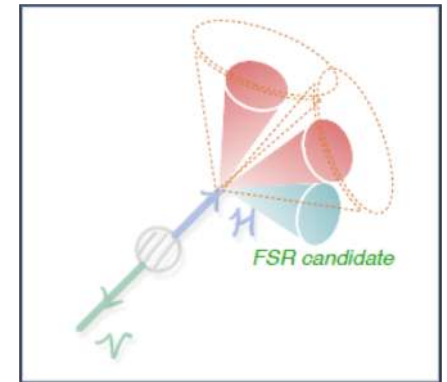


Charm-jet



FSR-jets recovery and $H \rightarrow cc$ reconstruction

- ❑ Higgs boson reconstructed using the two AK4 jets with highest CvsL scores
 - Energy regression is applied to the two Higgs jets
- ❑ FSR recovery used to further improve $m(H)$ resolution
 - Jets with $p_T < 20$ GeV, $|\eta| < 3$, and within $\Delta R < 0.8$ of Higgs jets are included in Higgs 4-momentum



Variable	Z($\nu\nu$)H	W($\ell\nu$)H	Z($\ell\ell$)H low- p_T (V)	Z($\ell\ell$)H high- p_T (V)
$p_T(V)$	> 170	> 100	[50 – 150]	> 150
$m_{\ell\ell}$	-	-	[75 – 105]	[75 – 105]
p_T^ℓ	-	(> 25(μ), > 30(e))	> 20	> 20
$p_T(j_1)$	> 60	> 25	> 20	> 20
$p_T(j_{two})$	> 35	> 25	> 20	> 20
$p_T(jj)$	> 120	> 100	-	-
$m(jj)$	< 250	< 250	< 250	< 250
$CvsL_{jone}$	> 0.225	> 0.225	> 0.225	> 0.225
$CvsB_{jtwo}$	> 0.40	> 0.40	> 0.40	> 0.40
N_{aj}	-	< 2	-	-
N_{al}	= 0	= 0	-	-
E_T^{miss}	> 170	-	-	-
METsig	-	> 4.0	-	-
Anti-QCD	Yes	-	-	-
$\Delta\phi(V, H)(rad)$	> 2.0	> 2.5	2.5	2.5
$\Delta\phi(pfMET, trkMET)(rad)$	< 0.5	-	-	-
$\Delta\phi(pfMET, lep)(rad)$	-	< 2.0	-	-

- ❑ Baseline selections shared with merged analysis
 - Resolved further split 2L:
 - High- p_T channel ($p_T(V) > 150$ GeV)
 - Low- p_T channel ($60 < p_T(V) < 150$ GeV)
- ❑ Additional event selections placed based on tagger scores of leading Higgs Jet
 - $CvsL > 0.225$ and $CvsB > 0.4$

Signal extraction – BDT training in SRs

Variable	Description	0L	1L	2L
$m(H)$	H mass	✓	✓	✓
$p_T(H)$	H transverse momentum	—	✓	✓
$p_T(V)$	vector boson transverse momentum	—	✓	✓
$m_T(V)$	vector boson transverse mass	—	✓	—
p_T^{miss}	missing transverse momentum	✓	✓	—
$p_T(V)/p_T(H)$	ratio between vector boson and H transverse momenta	✓	✓	✓
$CvsL_{max}$	$CvsL$ value of the leading $CvsL$ jet	✓	✓	✓
$CvsB_{max}$	$CvsB$ value of the leading $CvsL$ jet	✓	✓	✓
$CvsL_{min}$	$CvsL$ value of the subleading $CvsL$ jet	✓	✓	✓
$CvsB_{min}$	$CvsB$ value of the subleading $CvsL$ jet	✓	✓	✓
p_{Tmax}	p_T of the leading $CvsL$ jet	✓	✓	✓
p_{Tmin}	p_T of the subleading $CvsL$ jet	✓	✓	✓
$\Delta\phi(V, H)$	azimuthal angle between vector boson and H	✓	✓	✓
$\Delta R(j_1, j_2)$	ΔR between leading and subleading $CvsL$ jets	—	✓	✓
$\Delta\phi(j_1, j_2)$	azimuthal angle between leading and subleading $CvsL$ jets	✓	✓	—
$\Delta\eta(j_1, j_2)$	difference in pseudorapidity between leading and subleading $CvsL$ jets	✓	✓	✓
$\Delta\phi(\ell_1, \ell_2)$	azimuthal angle between leading and subleading p_T leptons	—	—	✓
$\Delta\eta(\ell_1, \ell_2)$	difference in pseudorapidity between leading and subleading p_T leptons	—	—	✓
$\Delta\phi(\ell_1, j_1)$	azimuthal angle between leading p_T lepton and leading $CvsL$ jet	—	✓	—
$\Delta\phi(\ell_2, j_1)$	azimuthal angle between subleading p_T lepton and leading $CvsL$ jet	—	—	✓
$\Delta\phi(\ell_2, j_2)$	azimuthal angle between subleading p_T lepton and subleading $CvsL$ jet	—	—	✓
$\Delta\phi(\ell_1, p_T^{miss})$	azimuthal angle between leading p_T lepton and missing transverse momentum	—	✓	—
$\Delta\eta(\ell_1, t)$	difference in pseudorapidity between leading p_T lepton and b-tagged jet from top quark decay	—	✓	—
$\Delta\phi(\ell_1, t)$	azimuthal angle between leading p_T lepton and b-tagged jet from top quark decay	—	✓	—
$\Delta R(\ell_1, t)$	ΔR between leading p_T lepton and b-tagged jet from top quark decay	—	✓	—
$CvsL_t$	$CvsL$ value of the b-tagged jet from top quark decay	—	✓	—
$CvsB_t$	$CvsB$ value of the b-tagged jet from top quark decay	—	✓	—
$P(b+bb)_t$	$DeepJet$ $prob(b+bb)$ value of the b-tagged jet from top quark decay	—	✓	—
$m(t)$	Reconstructed top quark mass	—	✓	—
$N_{small-R}^{nj}$	Number of small-R additional jets after the FSR subtraction	—	✓	—
$\sigma_{cReg}(j_1)$	leading p_T jet resolution from c-jet energy regression	✓	✓	✓
$\sigma_{cReg}(j_2)$	subleading p_T jet resolution from c-jet energy regression	✓	✓	✓
$\Delta\eta(V, H) _{kinfit}$	difference in pseudorapidity between vector boson and H, after kinematic-fit	—	—	✓
$\Delta\phi(V, H) _{kinfit}$	azimuthal angle between vector boson and H, after kinematic-fit	—	—	✓
$m(H) _{kinfit}$	H mass after kinematic-fit	—	—	✓
$p_T(H) _{kinfit}$	H transverse momentum after kinematic-fit	—	—	✓
$p_{Tmax} _{kinfit}$	p_T of the leading $CvsL$ jet after kinematic-fit	—	—	✓
$p_{Tmin} _{kinfit}$	p_T of the subleading $CvsL$ jet after kinematic-fit	—	—	✓
$p_T(V)/p_T(H) _{kinfit}$	ratio between vector boson and H transverse momenta after kinematic-fit	—	—	✓
$\sigma(H) _{kinfit}$	H invariant mass resolution from kinematic fit	—	—	✓

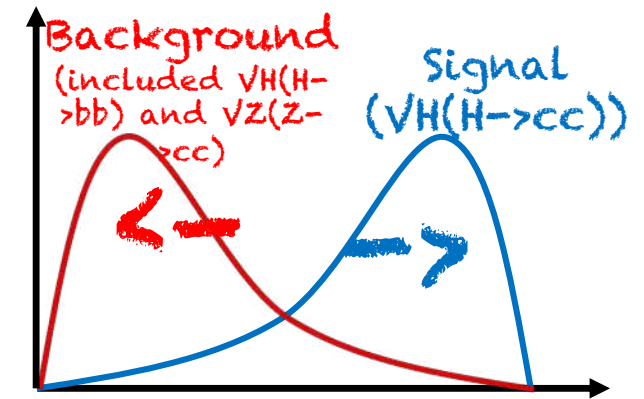
Higgs and vector boson properties

c-tagging score

event kinematics

Kinfit Variables (2L only)

- BDT trained to separate signal from background samples
 - Use combination of kinematic observables and particle flavor variables (tagger informations)
- Separate BDTs trained for each channel and data taking year
 - Separate BDTs trained for high- and low- $p_T(V)$ 2L
 - Variables used dependent on channel
- Reshaped BDT distribution used in SR during final fit



BDT score 48

Charm-tagging in the resolved-jet topology

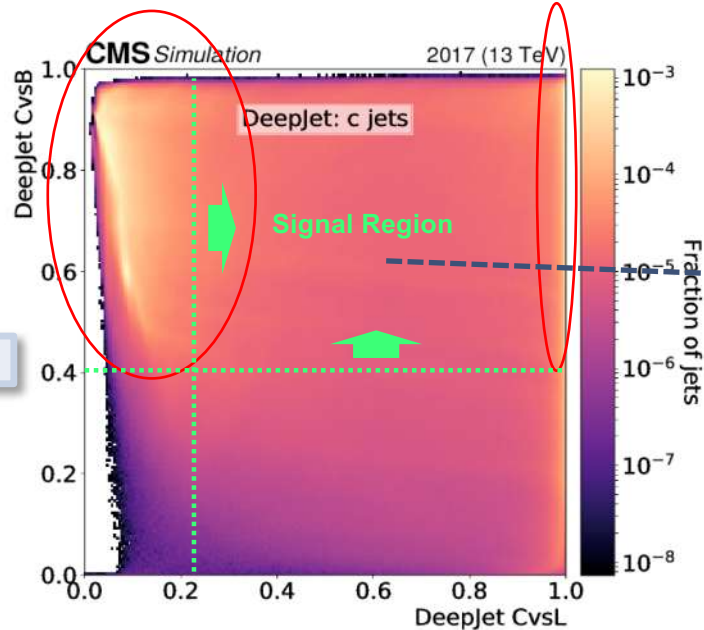
□ Definition of leading-jet working point

- Studies of CvsB/CvsL jet score distributions in 2D plane
- **CvsL > 0.225, CvsB > 0.4** → c-jet identification efficiency of ~43% with a b-jet and light-jet mis-tagging rate respectively of ~15% and ~4% (depending on the year)

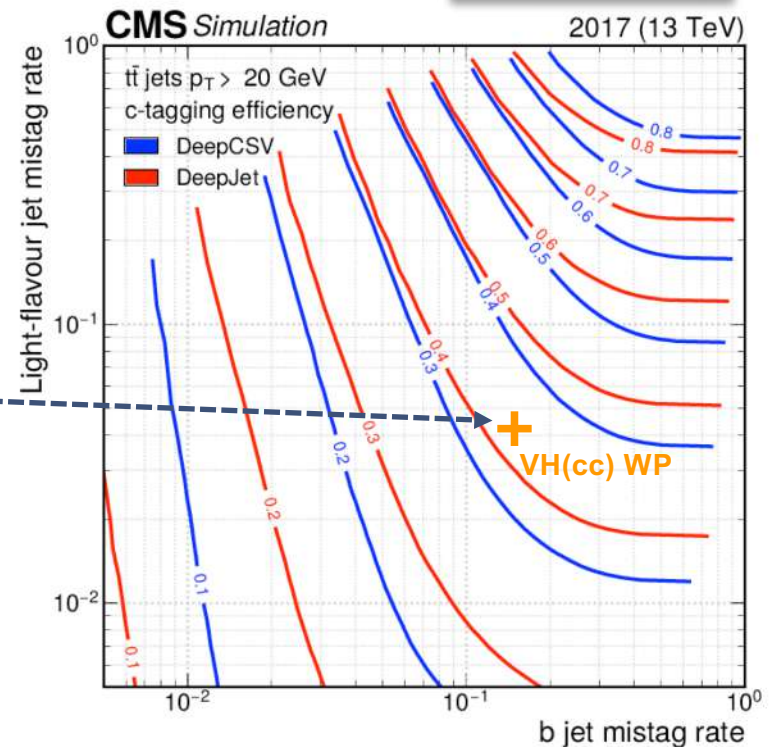
(from arXiv:2111.03027)

c-jets mis-identified as light ones

c-jets



(from arXiv:2111.03027)



A new method to calibrate charm-taggers

Methodology

- Iterative approach exploiting 3 distinct control regions, each enriched in b-jets, c-jets, or light-flavour jets

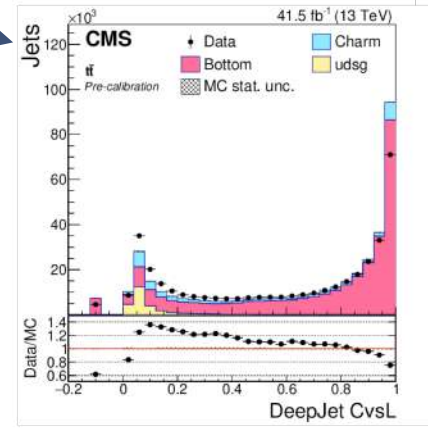
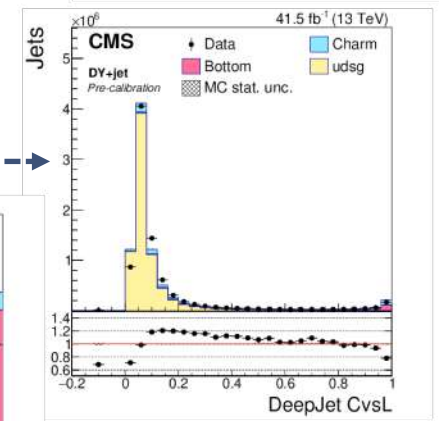
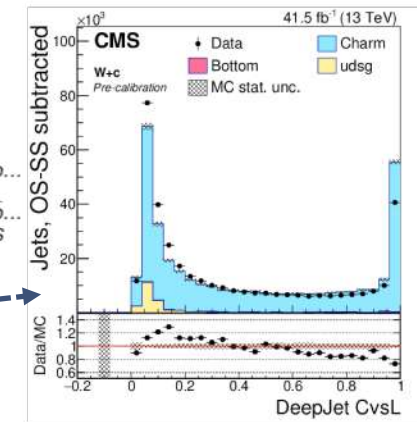
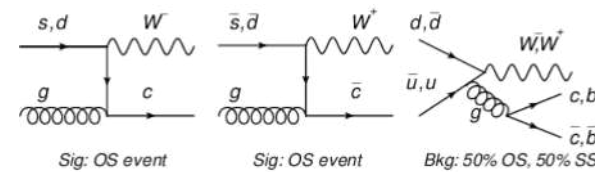
Selecting an abundant and pure source of charm-jets

- Target W production in association with charm quarks ($W+c$)
- Major background has 50% chance to have SS or OS final states
 - performing an OS-SS subtraction reduces considerably the W +gluon process
- To enrich in b-jets and light-jets: semi-(di-)leptonic $t\bar{t}$ +jets and $DY(Z\rightarrow\mu\mu/ee)$ +jets

- First time that a calibration method to correct the 2D distribution of c-tagging discriminator shapes is presented

→ [arXiv:2111.03027](https://arxiv.org/abs/2111.03027) (accepted by JINST)

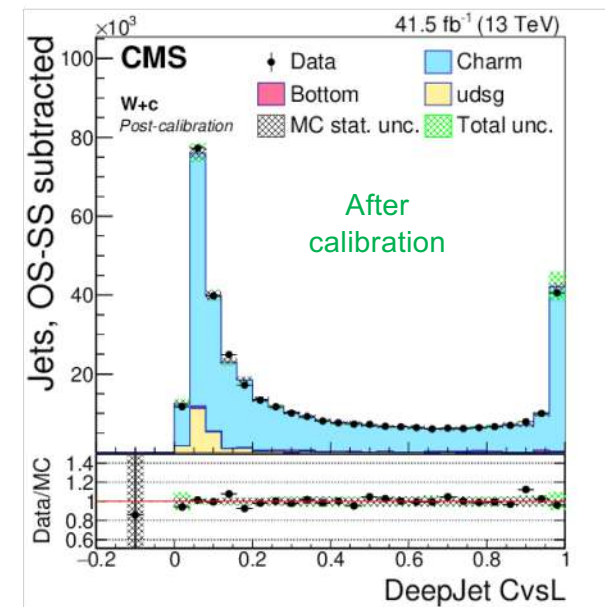
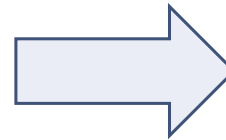
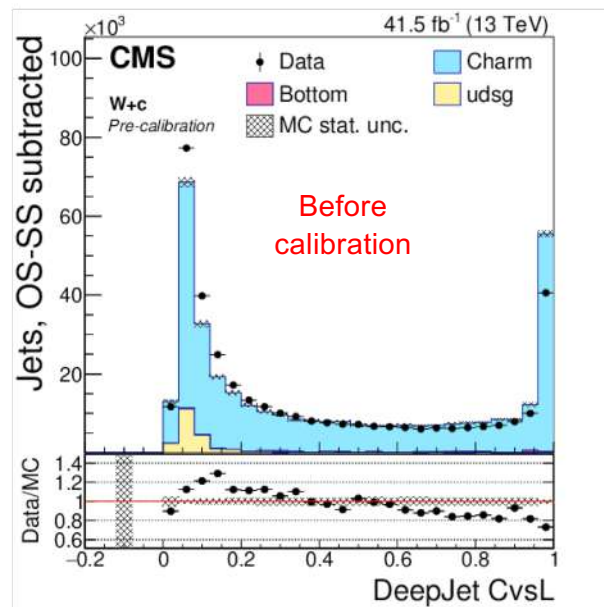
(from arXiv:2111.03027)



A new method to calibrate charm-taggers

Application of the reshaping scale-factors

(from [arXiv:2111.03027](https://arxiv.org/abs/2111.03027))



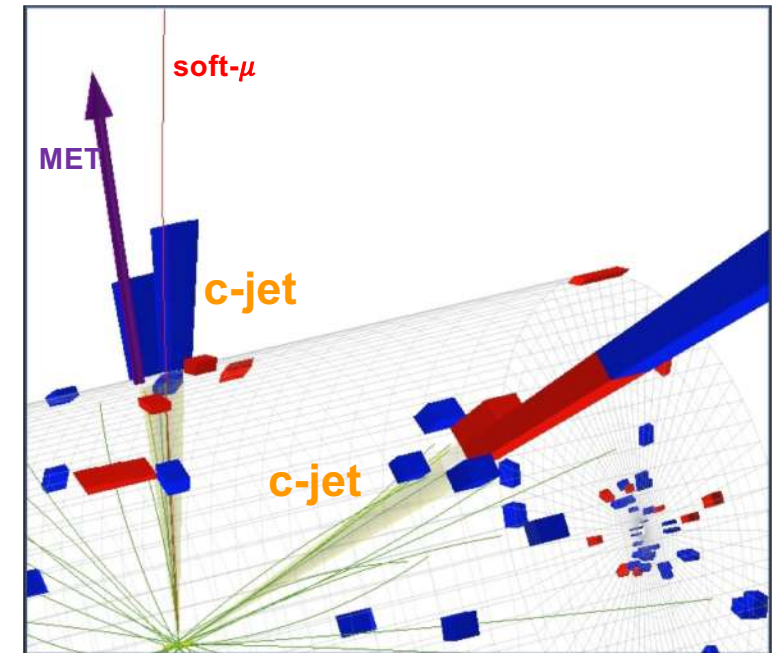
- Very good data/MC agreement after the calibration

- Application through an event-by-event re-weighting: $w_i = \prod_{i=1}^{jets} sf_i(CvsL, CvsB)$

A dedicated charm-jet energy regression

Goal: improve c-jet energy scale and resolution

- ❑ Inspired by b-jet energy regression [[arXiv:1912.06046](https://arxiv.org/abs/1912.06046)]
 - Jet energy measurements not always accurate:
 - neutrinos, hadrons outside jet radius, etc. Effect enhanced in c-jets and b-jets
 - Dedicated algorithm to determine c-jet energy scale and resolution
 - A DNN algorithm pioneered for the observation of the $H \rightarrow bb$ decay
- ❑ Regression performed using DNN architecture:
 - Trained using c-jets collected from $W \rightarrow cq$ decays in $t\bar{t}$ +jets MC events
 - Target is represented by $p_T(\text{gen})/p_T(\text{reco})$
- ❑ Input features
 - Total of 43 input variables as input to the network
 - Jets: kinematics, energy fraction, leading+soft-lepton tracks, pile-up, secondary vertices
 - Jet energy shapes (e.g. energy fraction, etc), jet constituents, $p_T(\text{jet})/p_T(\text{lepton})$

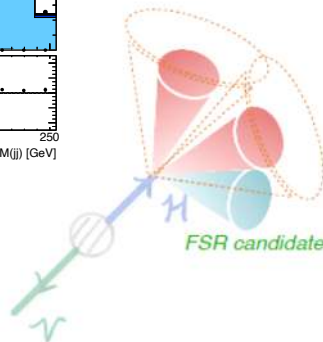
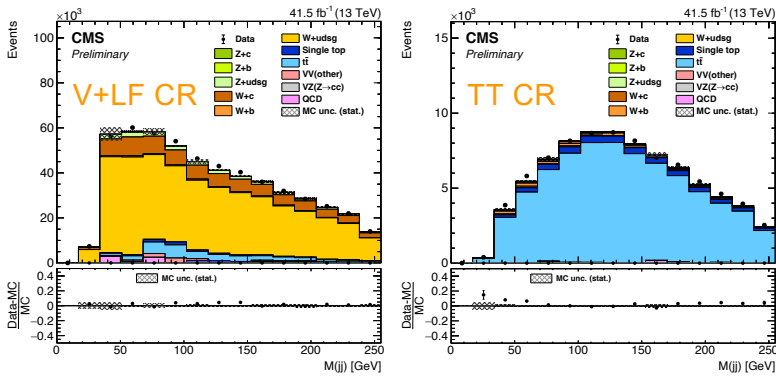


A dedicated charm-jet energy regression

~15% improvement in mass resolution

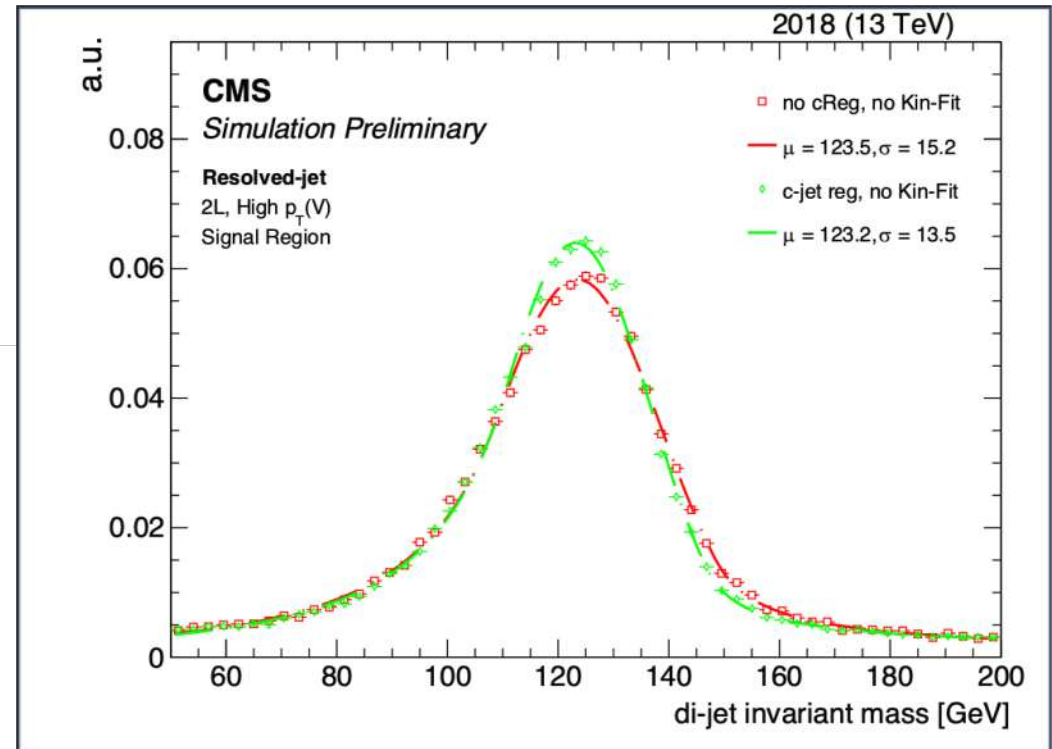
- Depending on the jet p_T

Validated in VH(H→cc) control regions



FSR recovery

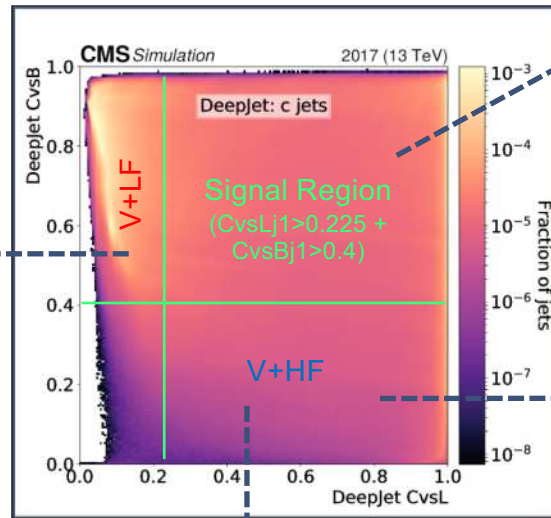
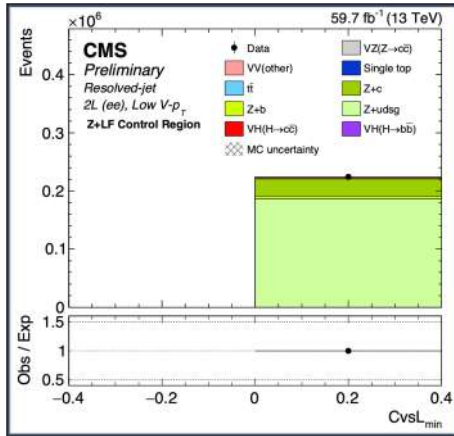
- Further improve di-jet invariant mass resolution
- Jets with $p_T < 20$ GeV, $|\eta| < 3$, and within $\Delta R < 0.8$ of Higgs jets are included in Higgs 4-momentum



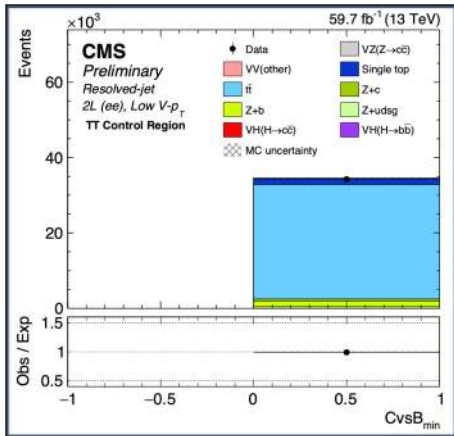
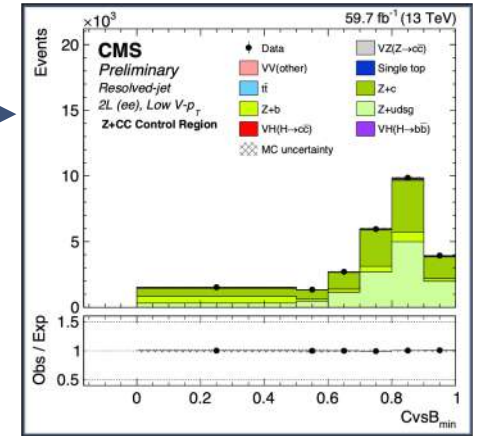
Background estimation – Resolved-jet

Accurate modeling of jet flavor in V+Jet background is vital for proper signal extraction

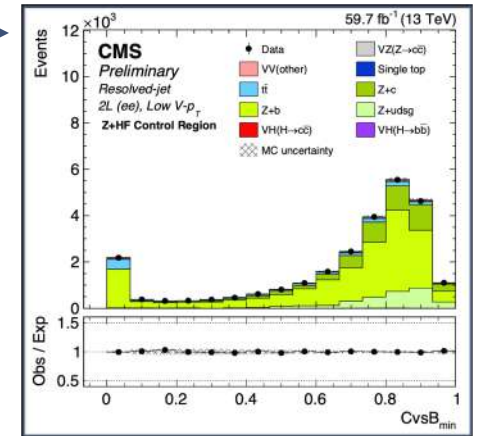
- Separate rate parameters for **V+c**, **V+b**, and **V+light** processes (no W+b)
- Additional rate parameter for $t\bar{t}$ background



V+CC
(\bar{c})
Veto $m(H)$
region



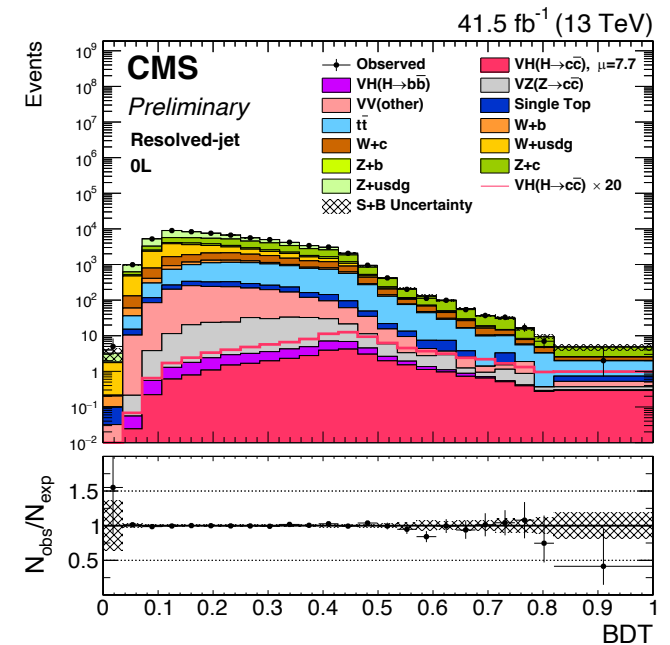
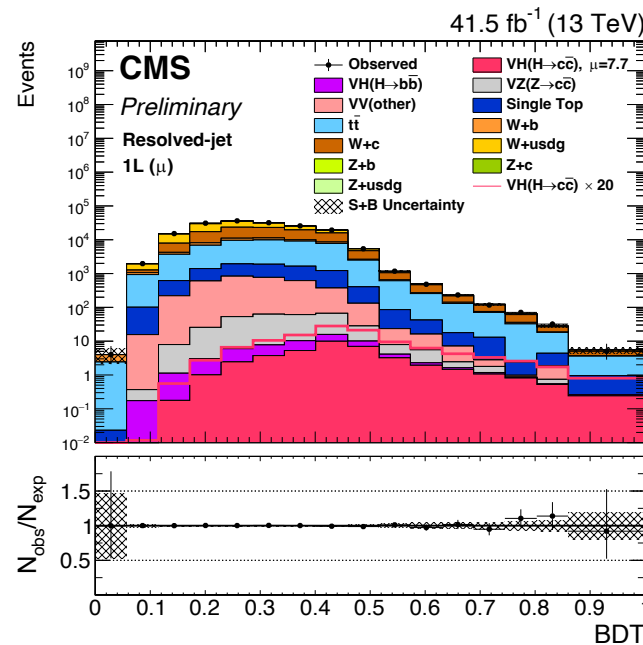
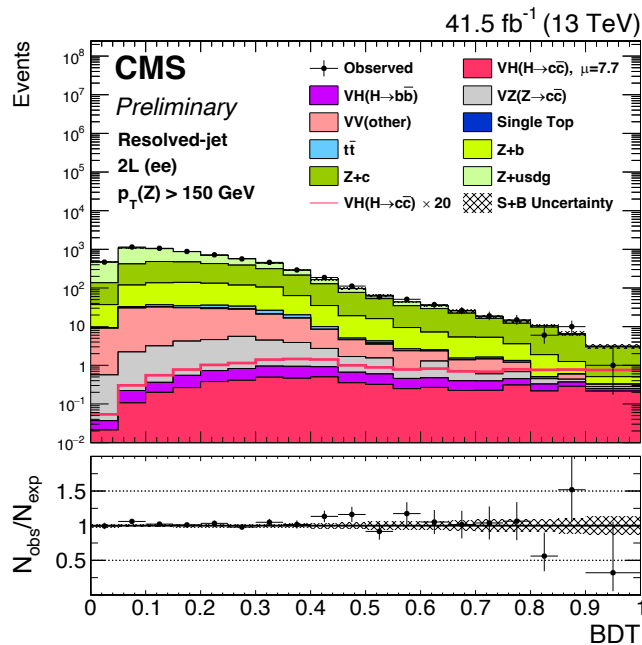
$t\bar{t}$
(\bar{c})
Invert Z mass (2L)
Require add jet (1L)*
Require add ℓ and jets (0L)



*1L: also require MET < 170 GeV to keep orthogonal to 0L $t\bar{t}$ CR

Postfit plots – Signal regions

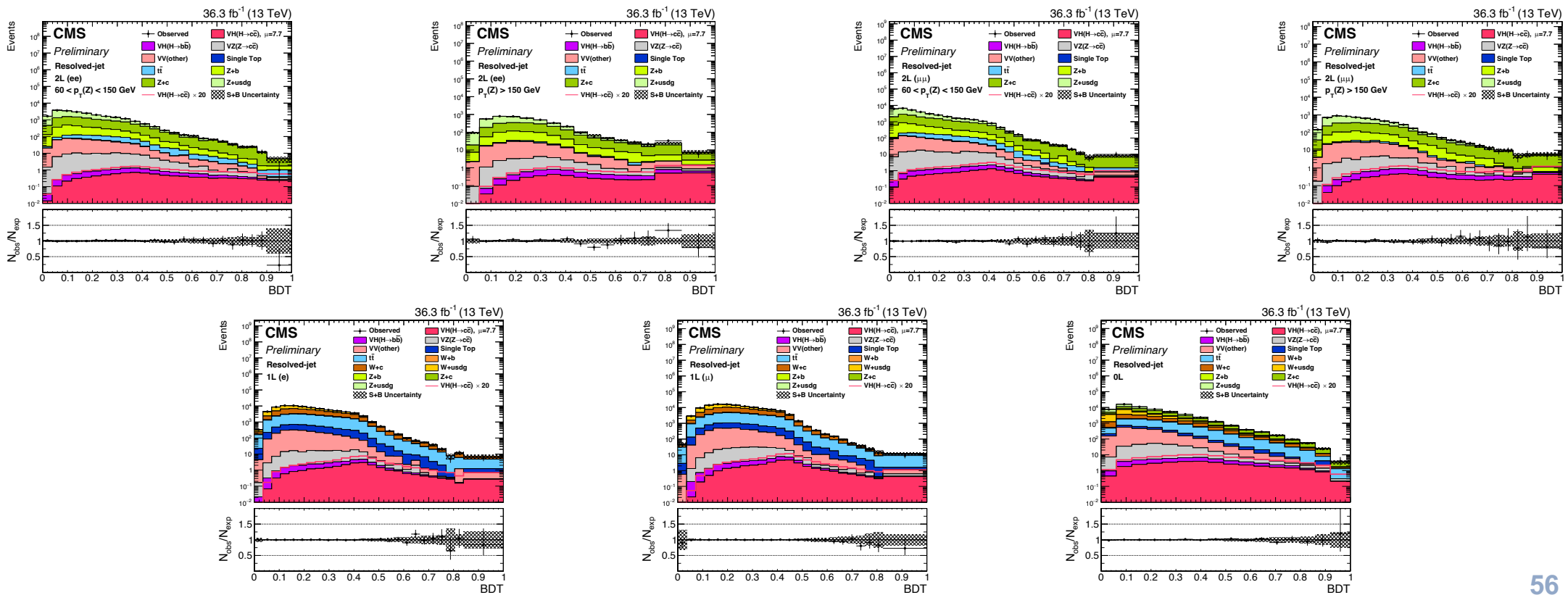
- Postfit distribution of the BDT discriminant obtained with the 2017 data (more in the back-up)
 - 7 Signal regions in each year: 2L(ee/ $\mu\mu$) Low- $p_T(V)$ and High- $p_T(V)$, 1L(e/ μ), and 0L



Postfit plots – Signal regions - 2016

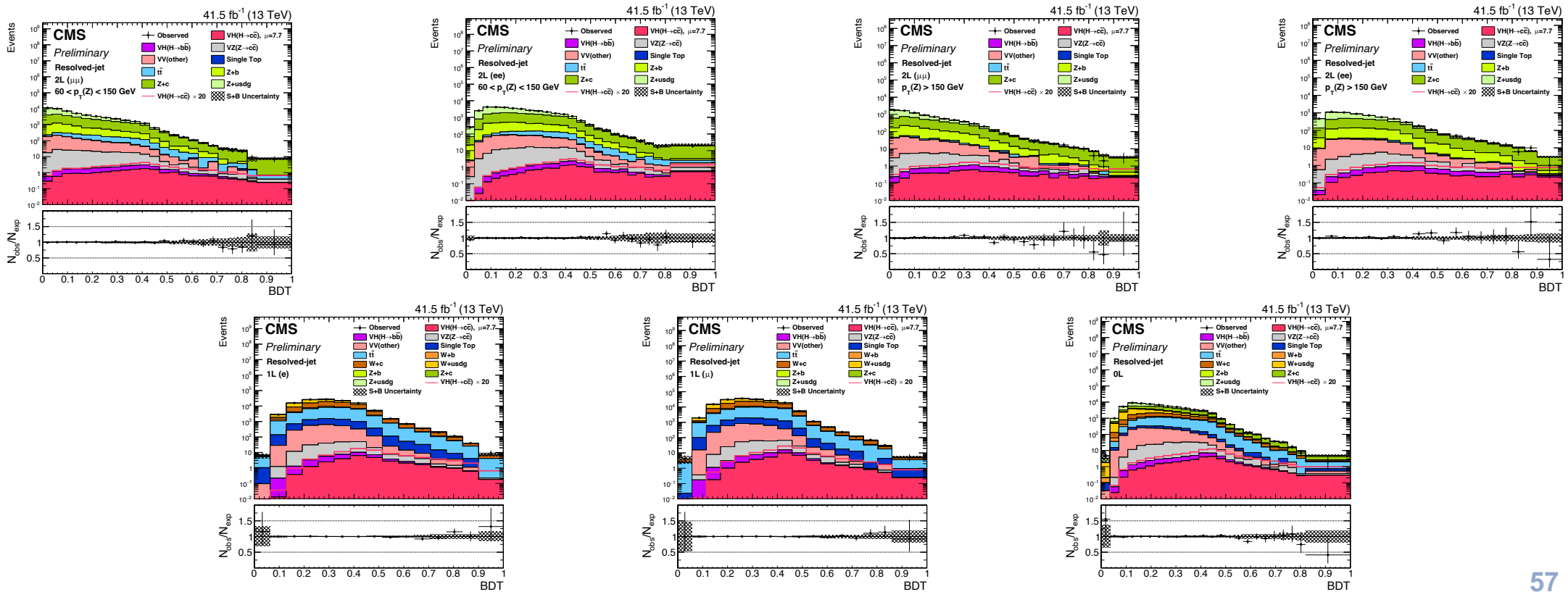
Postfit distribution of the BDT discriminant obtained with the 2016 data

7 Signal regions in each year: 2L(ee/ μ) Low- $p_T(V)$ and –High- $p_T(V)$, 1L(e/ μ) and 0L



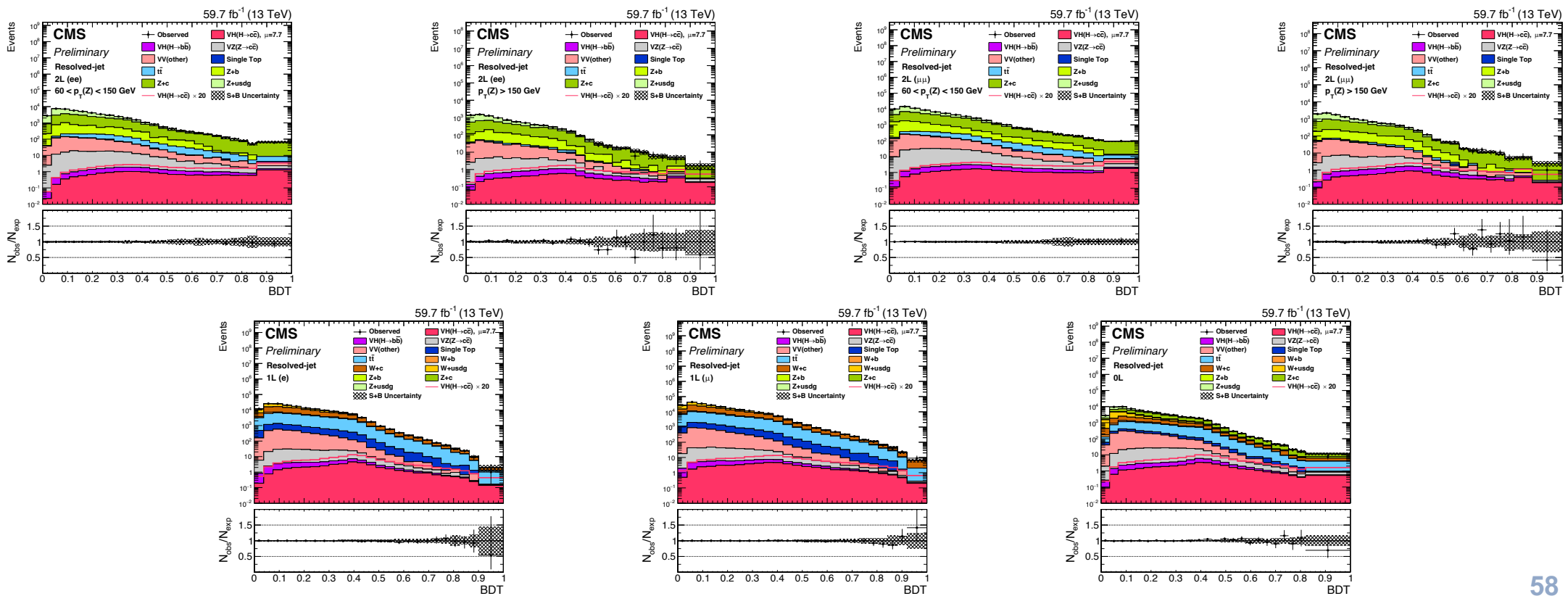
Postfit plots – Signal regions - 2017

- Postfit distribution of the BDT discriminant obtained with the 2017 data
 - 7 Signal regions in each year: 2L(ee/ μ) Low- $p_T(V)$ and –High- $p_T(V)$, 1L(e/ μ) and 0L



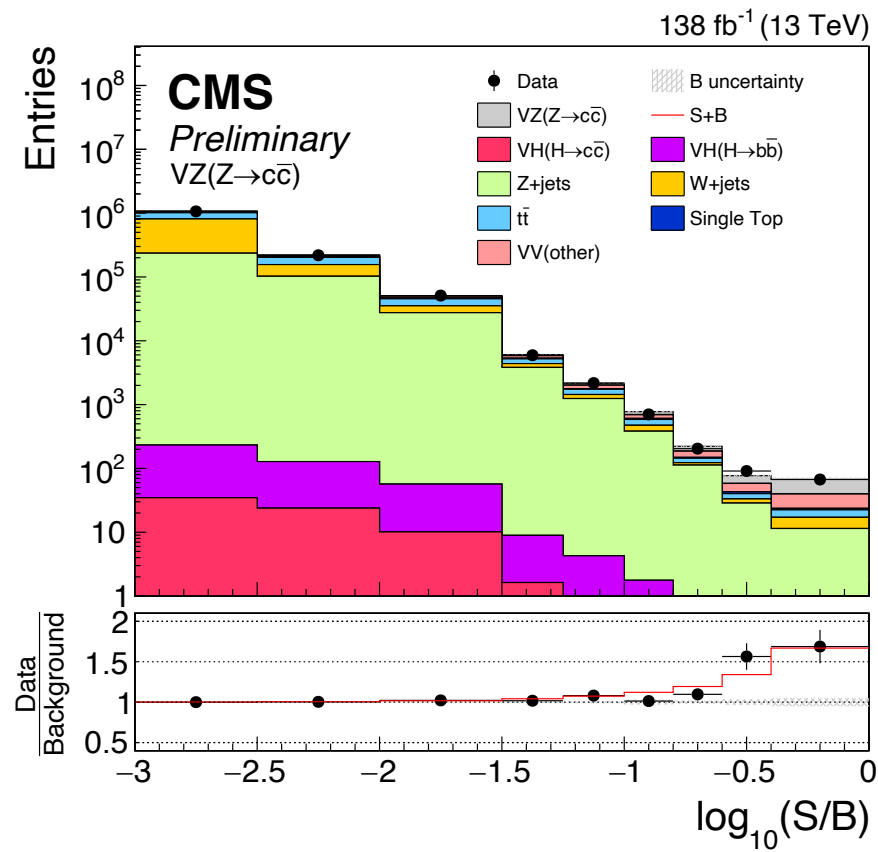
Postfit plots – Signal regions - 2018

- Postfit distribution of the BDT discriminant obtained with the 2018 data
 - 7 Signal regions in each year: 2L(ee/ μ) Low- $p_T(V)$ and –High- $p_T(V)$, 1L(e/ μ) and 0L



VZ(Z→cc) results

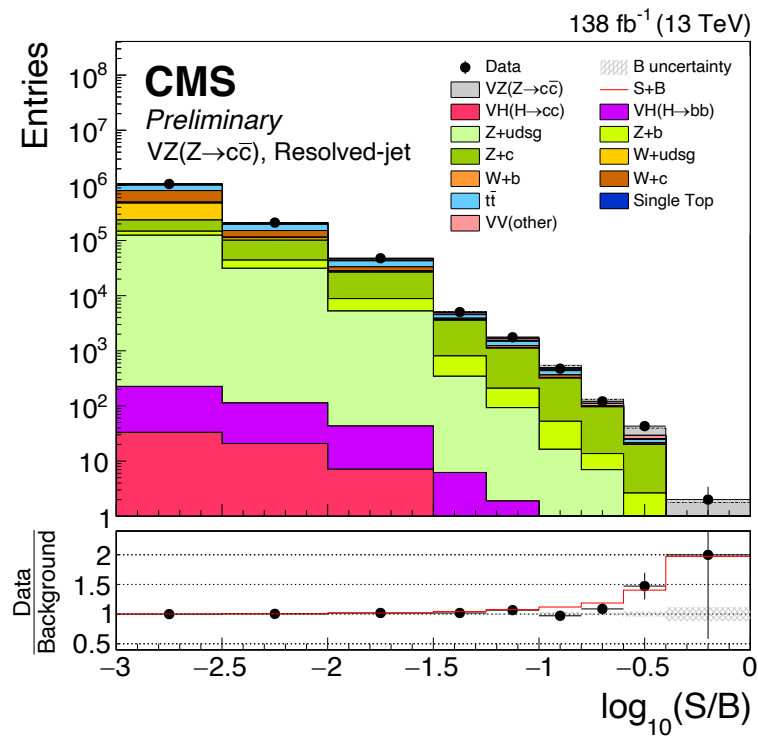
- Observing the excess: **distribution of events ordered by $\log_{10}(S/B)$**



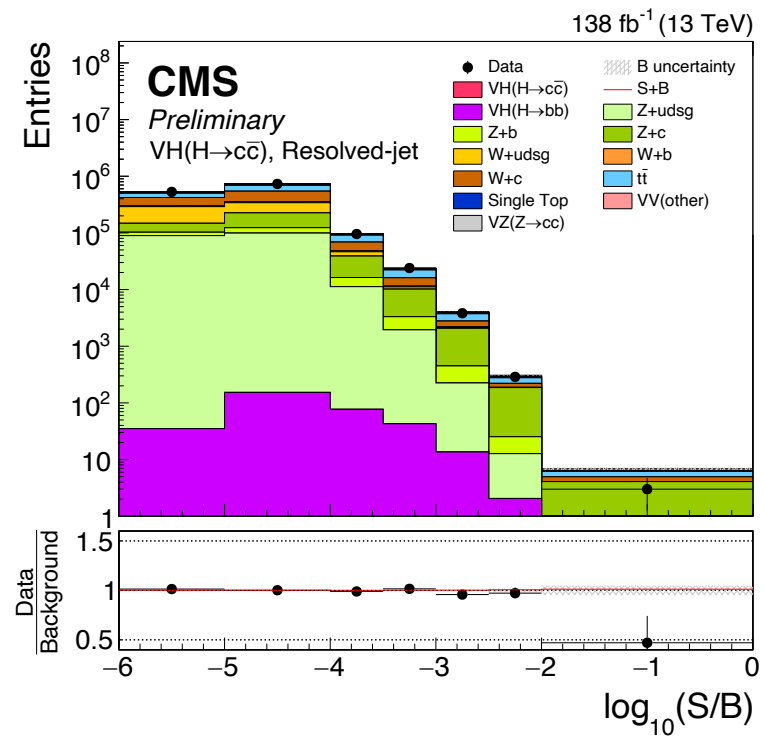
Resolved-jet topology - results

- Resolved-jet – all categories: **ordering the events by $\log_{10}(S/B)$**

VZ(cc)



VH(cc)



Background normalization scale-factors

- Simultaneous fit to BDT in SR and tagger shapes in CRs
 - CvsL of CvsL-subleading jet in V+LF CR
 - CvsB of CvsL-subleading jet in V+HF, V+CC, and TT CRs
- Allow V+c, V+b, V+udsg, and $t\bar{t}$ SFs to float freely in each channel
 - Z+x rate parameters independent of channel
 - 1L and 0L channels share W+c and W+udsg rate parameters

	Year	Z+c	Z+b	Z+light	W+c	W+light	$t\bar{t}$
2L-High	2016	0.90 ± 0.07	0.99 ± 0.06	1.04 ± 0.05	—	—	0.95 ± 0.05
	2017	1.12 ± 0.08	1.21 ± 0.08	0.94 ± 0.05	—	—	0.96 ± 0.05
	2018	1.19 ± 0.09	1.22 ± 0.09	0.94 ± 0.06	—	—	0.99 ± 0.05
2L-Low	2016	0.81 ± 0.06	0.83 ± 0.05	1.05 ± 0.05	—	—	0.89 ± 0.04
	2017	0.96 ± 0.07	0.94 ± 0.06	0.98 ± 0.05	—	—	0.90 ± 0.04
	2018	1.18 ± 0.14	1.04 ± 0.08	0.95 ± 0.05	—	—	0.92 ± 0.05
1L	2016	—	—	—	0.97 ± 0.06	1.04 ± 0.04	0.93 ± 0.04
	2017	—	—	—	1.04 ± 0.07	1.04 ± 0.05	1.08 ± 0.05
	2018	—	—	—	1.20 ± 0.07	0.93 ± 0.05	1.05 ± 0.05
0L	2016	0.96 ± 0.12	1.16 ± 0.20	1.28 ± 0.09	0.97 ± 0.06	1.04 ± 0.04	0.83 ± 0.05
	2017	1.31 ± 0.17	1.28 ± 0.22	1.03 ± 0.09	1.04 ± 0.07	1.04 ± 0.05	1.13 ± 0.07
	2018	1.14 ± 0.12	0.90 ± 0.20	0.89 ± 0.07	1.20 ± 0.07	0.93 ± 0.05	1.00 ± 0.07

Combination – VZ(cc) results

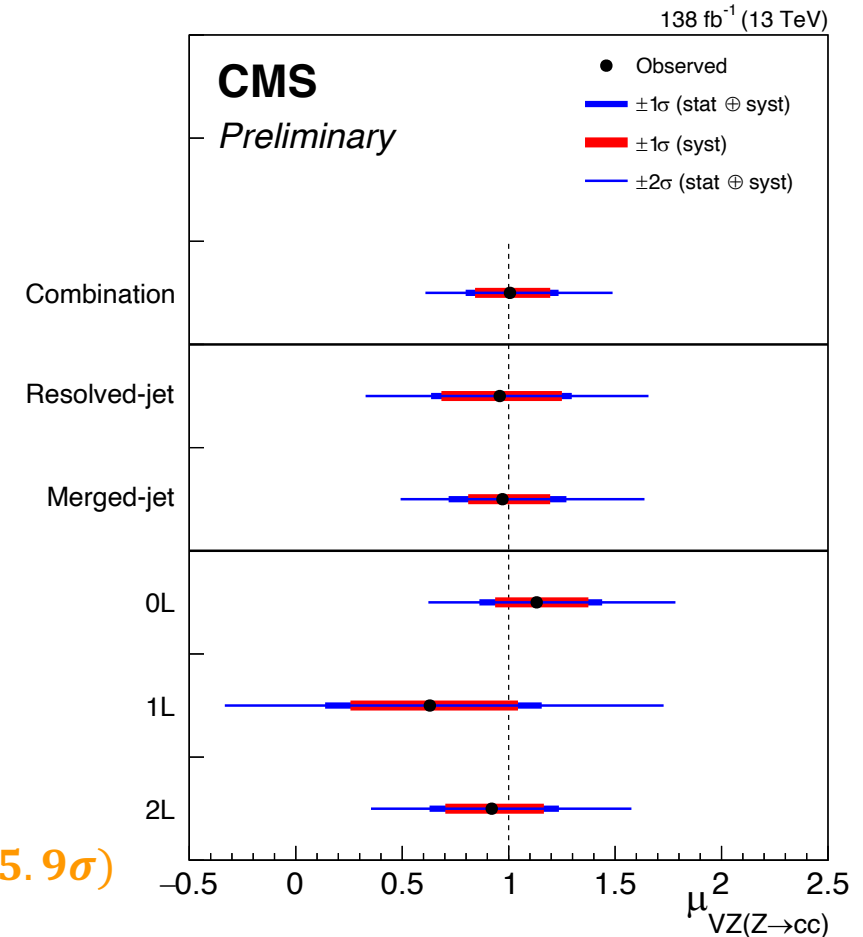
- Analysis validated by first looking for VZ(Z→cc) process
 - Same analysis procedure but extracting VZ(cc) signal during final fit
 - Resolved:** Use separate BDTs retrained with VZ(cc) as signal
 - VH(cc) fixed to SM expectation

	resolved-jet	merged-jet	combination				$\mu_{VZ(Z\rightarrow c\bar{c})}$
	($p_T(H) < 300$ GeV)	($p_T(H) \geq 300$ GeV)	0L	1L	2L	all	
2016 (expected)	1.7 σ	2.4 σ	2.5 σ	1.0 σ	1.9 σ	3.0 σ	1.00 ^{+0.42} _{-0.36}
2016 (observed)	1.8 σ	2.0 σ	3.6 σ	1.0 σ	0.4 σ	2.9 σ	1.02 ^{+0.41} _{-0.37}
2017 (expected)	2.2 σ	2.9 σ	2.9 σ	1.3 σ	2.6 σ	3.7 σ	1.00 ^{+0.35} _{-0.30}
2017 (observed)	1.7 σ	2.6 σ	1.3 σ	0.0 σ	4.0 σ	3.2 σ	0.84 ^{+0.32} _{-0.28}
2018 (expected)	1.7 σ	3.0 σ	3.1 σ	1.4 σ	2.0 σ	3.6 σ	1.00 ^{+0.39} _{-0.32}
2018 (observed)	1.9 σ	3.1 σ	4.0 σ	1.4 σ	1.2 σ	3.8 σ	1.23 ^{+0.45} _{-0.37}
Full Run2 (expected)	3.3 σ	4.7 σ	4.8 σ	2.1 σ	3.7 σ	5.9 σ	1.00 ^{+0.22} _{-0.20}
Full Run2 (observed)	3.1 σ	4.4 σ	4.9 σ	1.3 σ	3.3 σ	5.7 σ	1.01 ^{+0.23} _{-0.21}

- Measure observed (expected) signal strength of:

$$\mu_{VZ(cc)} = 1.01_{-0.21}^{+0.23} (1.00_{-0.20}^{+0.22}) \text{ with significance of } 5.7\sigma (5.9\sigma)$$

- First observation of Z→cc at hadron collider!**



Combination – VH(cc) results

Observed (expected) upper limit on VH(H → cc)

signal strength at 95% CL: $\mu_{VH(cc)} < 14 (7.6^{+3.4}_{-2.3})$

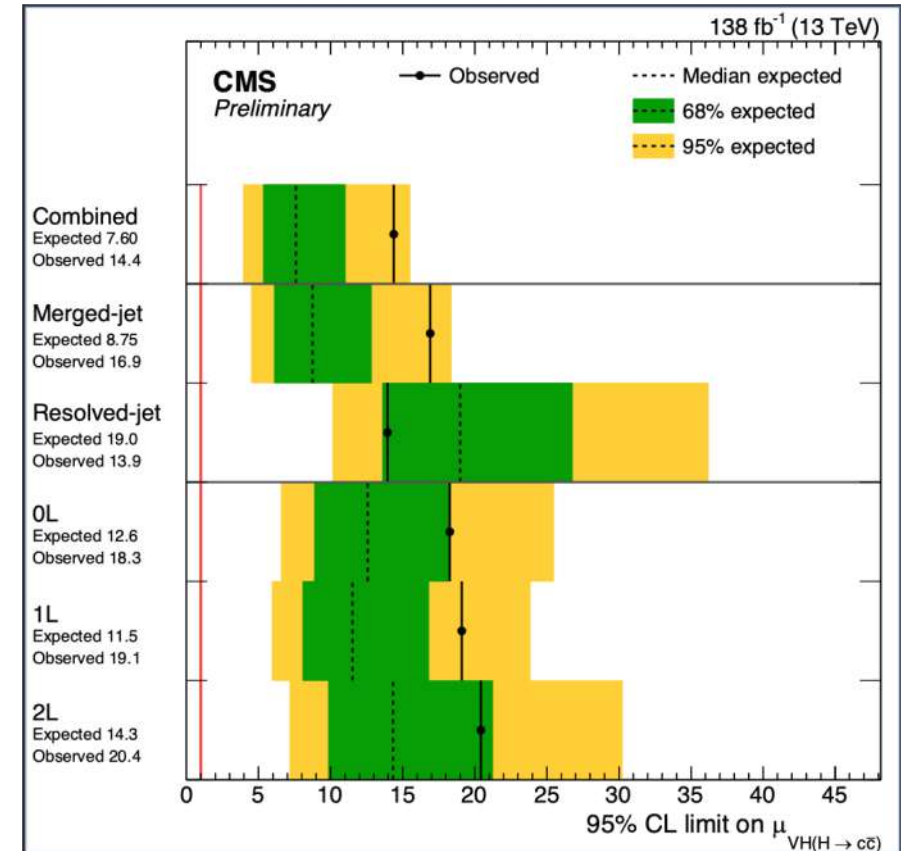
Strongest limits on the VH(cc) process to date!

ATLAS Full Run 2 result: $\mu_{VH(cc)} < 26 (31)$
[arXiv:2201.11428]

Best fit signal strength $\mu_{VH(cc)} = 7.7^{+3.8}_{-3.5} (+8.1, -6.6) (2\sigma)$

Consistent with the Standard Model prediction within 2σ

	resolved-jet	merged-jet	combination					$\mu_{VH(H \rightarrow c\bar{c})}$
	$(p_T(H) < 300 \text{ GeV})$	$(p_T(H) \geq 300 \text{ GeV})$	0L	1L	2L	all		
2016 (expected)	34	19	26	25	30	16	$1.0^{+7.6}_{-7.1}$	
2016 (observed)	28	20	21	43	21	18	$3.2^{+7.4}_{-7.3}$	
2017 (expected)	32	17	24	25	26	15	$1.0^{+6.9}_{-6.1}$	
2017 (observed)	24	24	29	26	31	18	$4.3^{+6.9}_{-6.2}$	
2018 (expected)	33	14	20	18	24	12	$1.0^{+5.6}_{-4.9}$	
2018 (observed)	26	26	34	18	42	21	$9.9^{+6.1}_{-5.1}$	
Full Run2 (expected)	19	8.8	13	12	14	7.6	$1.0^{+3.7}_{-3.4}$	
Full Run2 (observed)	14	17	18	19	20	14	$7.7^{+3.8}_{-3.5}$	



Obs. (Exp.) Run-2 single-analysis sensitivities:

Resolved: 14(19) xSM

Merged: 17(8.8) xSM

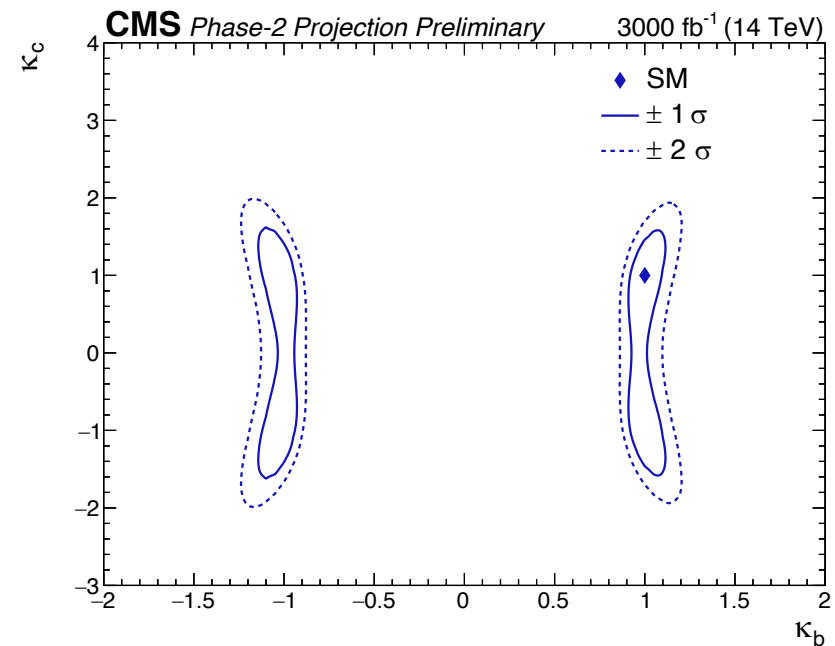
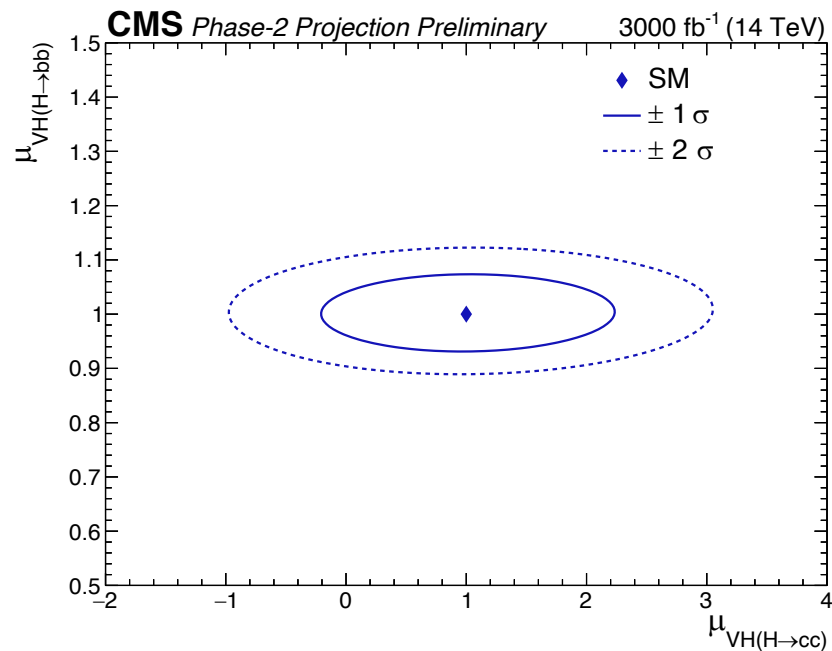
Projection at HL-LHC: Setup

- ❑ Extrapolation of the merged-jet analysis to HL-LHC with 3000 fb^{-1} data
- ❑ Modifications to the Run 2 analysis to allow for a simultaneous constraint on $H \rightarrow bb$ and $H \rightarrow cc$
 - **addition of 3 categories enriched in $H \rightarrow bb$ decays**, selected with the ParticleNet bb-tagging discriminant
 - very small (1-2%) overlap of bb and cc categories – events assigned to a unique category
 - **large-R jet p_T threshold lowered from 300 GeV to 200 GeV** – increasing signal acceptance
- ❑ Systematic uncertainties adjusted according to the Yellow Report [[CERN-2019-007](#)]
 - theoretical uncertainties: reduced by half
 - most experimental uncertainties: scaled down with $\sqrt{\mathcal{L}}$
 - bb and cc tagging efficiencies: constrained by $VZ(Z \rightarrow bb)$ and $VZ(Z \rightarrow cc)$ events to $\sim 3\%$ and $\sim 5\%$
 - misidentification of $H \rightarrow bb$ as $H \rightarrow cc$: a prominent uncertainty on $H \rightarrow cc$ measurement at HL-LHC
 - assumed to be reduced from $\sim 100\%$ (Run 2) to 20% in the projection

Projection at HL-LHC

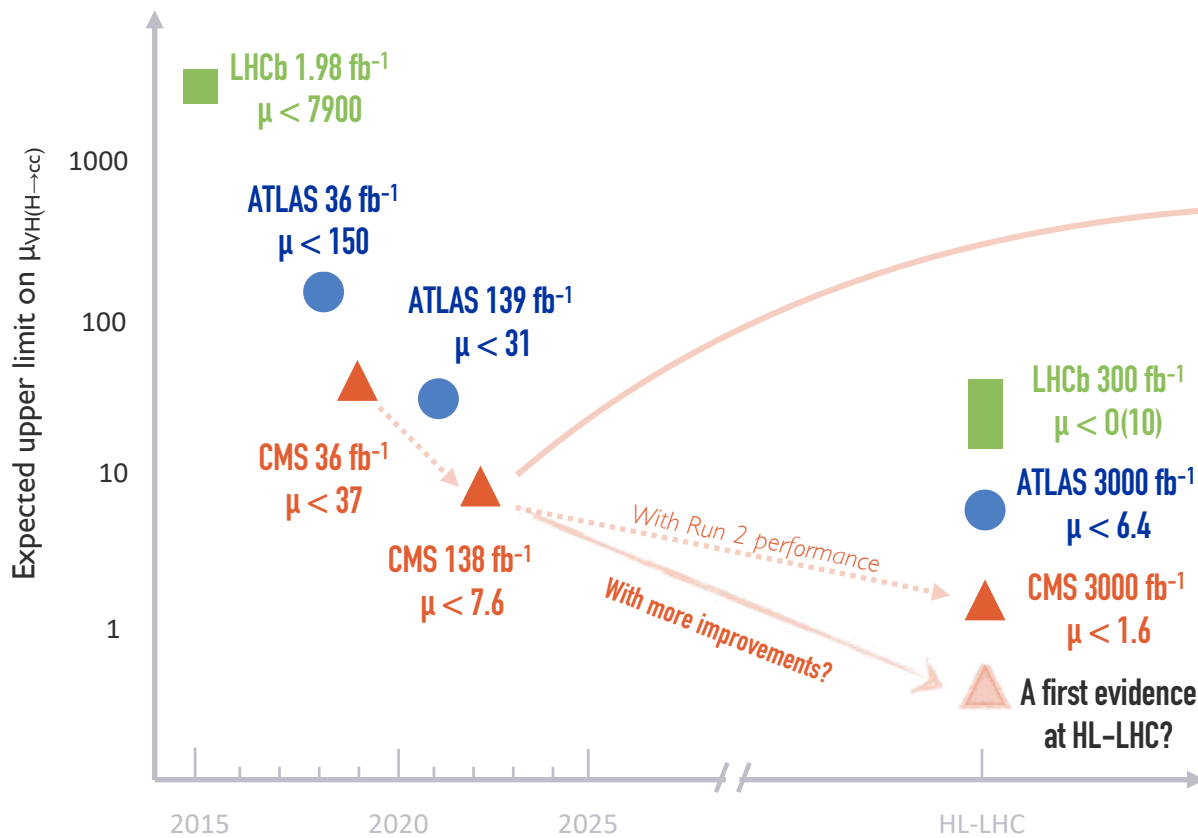
□ Simultaneous extraction of the $H \rightarrow bb$ and $H \rightarrow cc$ signal strengths

- $\mu_{VH(H \rightarrow bb)} = 1.00 \pm 0.03$ (stat.) ± 0.04 (syst.) = 1.00 ± 0.05 (total)
- $\mu_{VH(H \rightarrow cc)} = 1.0 \pm 0.6$ (stat.) ± 0.5 (syst.) = 1.0 ± 0.8 (total)

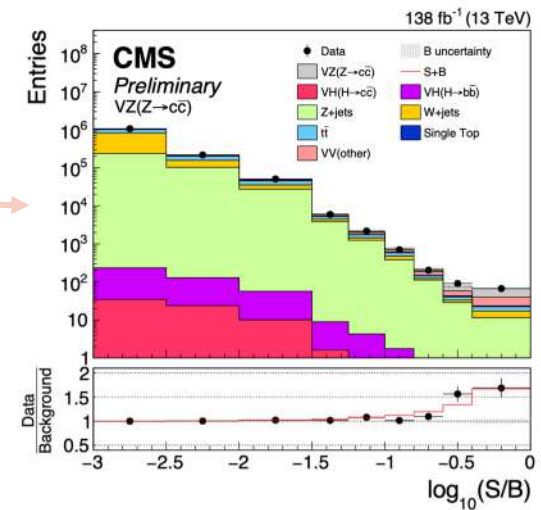


Expected sensitivity approaches the SM value for the Higgs-charm coupling.

A charming journey



From $\mathcal{O}(1000)$ to $\mathcal{O}(100)$ to $\mathcal{O}(10)$ in ~ 5 years.
 A combined effort and creativity from instrumentation,
 physics objects and analysis techniques!



First observation of $Z \rightarrow cc$ at a hadron collider!
 Opening a new era for future explorations.

- More channels: $t\bar{t}H(cc)$, VBF $H(cc)$, indirect constraints, etc.
- Improvements in advanced analysis techniques (e.g., Deep Learning) and instrumentation (e.g., tracker)
- Reduction of systematic uncertainties: c-tagging, event modeling, theoretical uncertainties, ...

A charming journey ahead!

Signal extraction – BDT training in SRs

- ❑ BDT trained to separate signal from background samples
 - Use combination of event kinematic observables, Higgs and vector boson properties, particle flavor variables (tagger information), and kinematic-fit variables (only in 2L channels)
- ❑ Separate BDTs trained for each channel and data taking year
 - Separate BDTs trained for high- and low- $p_T(V)$ 2L
 - Variables used dependent on channel
- ❑ Reshaped BDT distributions used in SR for the final fit

